Weathering of ordinary chondrites from Oman: Correlation of weathering parameters with ^{14}C terrestrial ages and a refined weathering scale

Florian J. ZURFLUH[1]*, Beda A. HOFMANN[1,2], Edwin GNOS[3], Urs EGGENBERGER[1] and A. J. Timothy JULL[4]

[1] Institut für Geologie, Universität Bern, Baltzerstrasse 1 + 3, CH-3012 Bern, Switzerland

[2] Naturhistorisches Museum der Burgergemeinde Bern, Bernastrasse 15, CH-3005 Bern, Switzerland

[3] Muséum d'histoire naturelle de la Ville de Genève, 1 Route de Malagnou, CP 6434 CH-1211 Genève 6, Switzerland

[4] NSF-Arizona AMS Laboratory, The University of Arizona, 1118 East Fourth St., Tucson, Arizona 85721, USA

* Corresponding author. E-mail address: zur0flo@gmail.com

Key words:

Weathering scale, meteorite weathering and contamination, ^{14}C terrestrial ages, handheld XRF, hot desert, Oman

Short title:

Weathering parameters of ordinary chondrites from Oman

Abstract

We have investigated 128 ^{14}C dated ordinary chondrites from Oman for macroscopically visible weathering parameters, for thin section based weathering degrees and for chemical weathering parameters as analyzed with handheld XRF (HHXRF). These 128 ^{14}C dated meteorites show an abundance maximum of terrestrial age at 19.9 ka, with a mean of 21.0 ka and a pronounced lack of samples between 0 and 10 ka. The weathering degree is evaluated in thin section using a refined weathering scale based on the current W0-W6 classification of Wlotzka (1993), with five newly included intermediate steps resulting in a total of nine (formerly six) steps. We find significant correlations between terrestrial ages and several macroscopic weathering parameters. The correlation of various chemical parameters including Sr and Ba with terrestrial age is not very pronounced. The microscopic weathering degree of metal and sulfides with newly added intermediate steps shows the best correlation with ^{14}C terrestrial ages, demonstrating the significance of the newly defined weathering steps. We demonstrate that the observed ^{14}C terrestrial age distribution can be modeled from the abundance of meteorites with different weathering degrees, allowing the evaluation of an age-frequency distribution for the whole meteorite population.

INTRODUCTION

The majority of meteorites available for scientific study are finds, affected to variable degree by terrestrial weathering. Most of these meteorites are recovered from hot deserts where weathering rates are lower than in more humid areas. Several studies have been performed to quantify terrestrial alteration of hot desert meteorites by Mössbauer spectroscopy (Bland et al. 1998), geochemical investigations (Al-Kathiri et al. 2005; Crozaz et al. 2003; Hezel et al. 2011) or iron isotope analyses (Saunier et al. 2010). Many of the applied methods for quantifying the amount of weathering are relatively expensive and time consuming and thus not applicable to large numbers of hot desert meteorites. To obtain weathering information for large collections (hundreds to thousands of samples), in this study we tested several schemes for the assessment of the degree of weathering. A need for relatively simple ways to quantify weathering by several methods was originally proposed by Gooding (1986) due to the large amounts of samples found in Antarctica. These meteorites are classified by a weathering index, using the macroscopically visible degree of rustiness into categories A, B and C (Cassidy 1980). For meteorites with evaporitic deposits a lower-case "e" was proposed (Velbel 1988). This scheme allows a rapid estimation of weathering, but the resulting classification is rather crude. Also, the physical meaning of the weathering categories is not clear (Gooding 1989; Ikeda and Kojima 1991; Losiak and Velbel 2011). When large numbers of meteorites were becoming discovered in hot deserts, classification of the weathering using thin sections was proposed, with scales ranging from A to C (Jull et al. 1990), A to E (Jull et al. 1991) or A to D (Jull et al. 1993). A slight modification was then proposed with weathering grades W0 to W6 (Wlotzka 1993). This system is currently in use for non-Antarctic meteorites. However, the original publication is an abstract containing limited details and several ambiguities. In this study we use a refined weathering scale, which is compatible with Wlotzka (1993), but additionally dividing grades W3 and W4 into three and two subgrades, respectively.

The determination of terrestrial ages is crucial for understanding of accumulation rates and weathering timescales. Meteorites from hot deserts survive shorter time spans than meteorites from Antarctica and can therefore be dated by the use of cosmogenic ^{14}C (e.g., Jull 2006).

Terrestrial age dating of meteorites also allows determining minimum ages of accumulation areas and geomorphological studies. If a large population from an accumulation area is dated, calculation of meteorite flux is possible (Bland et al. 1996; Zolensky et al. 2006). Since meteorites record conditions from the environment, paleoclimatic studies could be performed using meteorites since their pre-terrestrial composition is well-defined by falls and they are found in all areas on Earth (Bland 2006). One of the features recognized is the contamination of hot desert meteorites with terrestrial Sr and Ba (Al-Kathiri et al. 2005; Crozaz et al. 2003; Nazarov et al. 2004a; Saunier et al. 2010; Shih et al. 2002; Stelzner et al. 1999). Initial concentrations in ordinary chondrites are 9 to 11 µg/g Sr and 3 to 5 µg/g Ba (Wasson and Kallemeyn 1988). Even within some decades the concentrations of these elements can increase by a factor of two as observed in samples from the Holbrook 1912 fall collected in 1968 (Gibson and Bogard 1978). Previous studies of meteorites from Oman showed a correlation of weathering features including bulk geochemical parameters with ^{14}C terrestrial ages of meteorites (Al-Kathiri et al. 2005) and the common involvement of highly saline porewaters in the weathering process (Zurfluh et al. 2013). Samples from ancient meteorite showers usually show a wide variation in degree of weathering. Individuals from the large meteorite strewn field JaH 073 in central Oman (terrestrial age 14.4 ka based on ^{10}Be and ^{14}C data of several stones) vary from W2 to W4 (Gnos et al. 2009).
Access to many complete individuals of ordinary chondrites from Oman allowed us to perform studies on weathering and contamination including macroscopic, microscopic, environmental and chemical parameters and also to identify patterns that are dependent on local geography or geological situation. In this study, we investigate correlations between weathering parameters and ^{14}C terrestrial ages of ordinary chondrites from Oman.

SAMPLES AND ANALYSES

Ordinary chondrites from Oman

For this study, ordinary chondrites (OC) found in the hot desert of Oman by the Omani-Swiss meteorite search expeditions in the years 2001 to 2010 (Hofmann et al. 2004) were investigated. Some of these meteorites (found 2001 to 2003) were part of earlier research (Al-

Kathiri et al. 2005). Since the present investigation aims to show the variation of weathering and terrestrial ages of a whole meteorite population, samples from large meteorite showers like JaH 073 and JaH 091 also were used. Meteorites are carefully documented in the field including a description of the soil surface. Samples were packed without direct contact in polypropylene bags for transportation. During the unpacking process, gloves were worn to preclude contamination. The adhering soil was removed using pressurized air. Meteorites were cut using isopropanol and standard rectangular or round polished thin sections were prepared from representative parts of the meteorite samples. Usually, thin section chips were taken along profiles from exterior to interior of the meteorite including varnished surfaces. Meteorites usually weather from outside to inside. Larger meteorites often have relatively fresh "cores" and weathered outer parts. Representative parts are supposed to be samples from core and rim. Most of the samples originate from the transition of exposed towards buried areas. They were investigated under optical microscope and electron microscopes (scanning electron microscope, SEM with EDS: Zeiss EVO50 and electron microprobe, EMP: Jeol JX-8200).

Terrestrial age determination

Our first set of measurements included 50 ^{14}C analyses of meteorites selected on the base of weathering grade (Al-Kathiri et al. 2005). The next phase of our study involved 78 samples that were selected using the following criteria: (1) all individual samples found on the Jabin plateau (approximately 21° 0-24'N / 28° 22-26'E) west of the Wahibah sands in the meteorite recovery area Ramlat al Wahibah (RaW), an area underlain by lithified dune sands with a maximum age of about 120 ka (Preusser et al. 2002; Radies et al. 2004); (2) all LL chondrites of the campaigns from 2001 to 2009; and (3) selected samples covering a profile of around 300 km length from the Arabian sea to areas as distant from the sea as possible, including all stages of the modified weathering degree. Meteorites with masses between 200 g and 2000 g were selected. Samples from recognized strew fields were avoided since average ^{14}C saturation values used for the terrestrial age calculations are only valid for objects <100 to 150 cm in diameter. Exceptions are stones from the above-mentioned, well dated strewn fields JaH 073 and JaH 091. Large stony meteoroids typically have complex exposure histories and fragment during their atmospheric entry producing large strewn fields (e.g., Huber et al. 2008). Cosmogenic nuclide production rates are a function of depth, thus large meteoroids can only be dated reliably by using a combination of several cosmogenic isotope systems permitting to unravel complex exposure histories.

The terrestrial ages of the meteorites were calculated from the activity of cosmogenic ^{14}C in 0.04 g to 2.4 g (typically 0.5 g) subsamples of ordinary chondrites. Radiocarbon activities were analyzed using methods described elsewhere (Bland et al. 1998; Jull 2006; Jull et al. 1998; Jull et al. 1993; Jull et al. 1989; Jull et al. 1990). To remove terrestrial carbon, samples were cleaned with 85% phosphoric acid (to remove terrestrial carbonates) and heated to 500°C in air (to remove terrestrial low temperature components). All ^{14}C analyses were performed at the NSF-Arizona AMS Laboratory, University of Arizona, Tucson. The ages were calculated using ^{14}C production rates of 46.4 dpm/kg for H-chondrites, 51.1 dpm/kg for L-chondrites and 55.2 dpm/kg for LL-condrites, respectively. The upper age range depends on the detection limit for ^{14}C, which is dependent on sample size. Most analyses were performed on samples of 0.1 to 0.2 g for practical reasons (lifetime of extraction line), with detection limits of ~0.5 dpm/kg ^{14}C corresponding to 30 to 35 ka. Some of our earlier measurements were performed on rather large samples of up to 1 g, yielding a ^{14}C detection limit corresponding to ages of up to ~55 ka. For statistics we used the minimal ages of samples close to detection limit.

Description of macroscopic weathering features

Macroscopically visible weathering effects were estimated for all ^{14}C dated meteorites and all samples collected during field campaigns 2009 and 2010 using a simple intensity scale ranging from 0 to 3 for each parameter (Table 1, Fig. 1). The following parameters were determined: Wind ablation on exposed surface (ES); sand on ES; fusion crust on ES; salt efflorescence on cut surface (CS) (Zurfluh et al. 2013); pores and pore space filling on CS; secondary crack abundance; white mineral precipitations on buried surface (BS); staining with secondary green Ni-minerals (Al-Kathiri et al. 2005); abundance of lichen; degree of red coloration of BS as compares with ES (color difference established using the rock color chart, (Goddard 1948).

The surfaces of fresh meteorites are either black where fusion crust (FC) is present (N1 on Goddard scale) or grey on broken surfaces (N3-5). With increasing weathering, the alteration mineralogy is responsible for a dark, dusky brown color (5YR 2/2) of the meteorites. If a "red BS" evolves, the part of the meteorite buried in the soil attains a light brown color of 5YR (4-5)/6 or 5YR (3-5)/4 (Table 1, Fig.1d). All macroscopic weathering parameters are examined by naked eye and with the use of a binocular microscope. All samples were investigated independently by at least two persons to reduce personal bias.

Classification of weathering degree

The grade of weathering of meteorites is currently reported using thin-section observation and the scale defined by Wlotzka (1993). This classification scheme leaves some ambiguities in the definition of weathering steps, in particular W3 (Fig. 2a). Following Wlotzka (1993) W3 is defined as "heavy oxidation of metal and troilite, 60-95% being replaced". It remains unclear to what exactly the percentages refer. Because weathering degree W2 (Wlotzka 1993) just takes into account the oxidation of metal (maximum 60% oxidized), it is not clear where to place meteorites with >60% of metal and <60% of combined metal+troilite altered. It is generally straightforward to distinguish altered Fe-Ni metal from altered troilite (Fig. 3). This is particularly relevant because many meteorites recovered in Oman show metal oxidation close to 95 % while the degree of alteration of troilite is often much lower, about 20% (Fig. 2b). It is well established that metal is oxidized first in meteorites under hot desert conditions whereas the alteration of troilite is slower (e.g., Al-Kathiri et al. 2005; Lee and Bland 2004). There are only a few exceptions where troilite is weathered preferentially compared to metal. Examples are two L chondrites from Western Australia at initial stages of weathering (Bevan et al. 2001; Ruzicka 1995). Samples from Antarctica often show no or only minor alteration of troilite (Lee and Bland 2004). We therefore introduce intermediate steps to the weathering grades 3 and 4 and a more detailed description of the altered phase (Table 2). To avoid confusion with the Wlotzka scale, we suggest to indicate classifications based on our scale with one decimal numbers (e.g., W3.0). Due to the incomplete definition of the W2/W3-boundary by Wlotzka (1993) in the original publication, we consider the upper limit of W2 (60% metal oxidation) as the lower limit for W3 (Fig. 2b). W3 is further divided into W3.0, W3.3 and W3.6 corresponding to troilite oxidation degrees of <20%, 20-60% and >60%, respectively. The boundary to W4 remains at 95% oxidation of metal and 95% oxidation of troilite. We include an additional extension W4.5 to account for samples where essentially no metal and troilite is left (if not fully enclosed in silicates). The Wlotzka (1993) definition of W5 is problematic, as we often observe beginning alteration of mafic silicates in samples belonging to W3 based on metal and troilite oxidation (Fig. 3). In the collection of ~880 unpaired samples found in Oman we have only one sample classified as W5.0. Stage W6.0 was not observed among our finds from Oman and is adopted unmodified (Table 2).

W3 actually comprises the major part of the alteration history of ordinary chondrites. Most importantly, our refined scale for weathering degree classification is compatible with the official scale (Wlotzka 1993), for example, a previous W3 meteorite will remain at the same stage but could be either a W3.0, W3.3 or W3.6 (Fig. 2b). The stages W0, W1 and W2 were adopted unmodified. To take also into account the possible preferred weathering of troilite as observed in Australian chondrites (Bevan et al. 2001; Ruzicka 1995) further division of weathering stages W1 and W2 (analogous to W3 into W3.0, W3.3 and W3.6) might be applied (Fig. 2b).

For the calculation of correlations, each step of the weathering degrees was treated independently with a number assigned, i.e. W0.0 = 0 to W6.0 = 9.

Quantification of terrestrial elemental contamination

All ^{14}C dated meteorites were non-destructively analyzed for their elemental composition with a Thermo Scientific NITON XL3t-600 handheld energy dispersive X-ray Fluorescence (HHXRF) analyzer placed in a mobile test stand. To obtain proper results for meteorites a slightly adjusted calibration of the “mining mode” was used (Zurfluh et al. 2011). Elements analyzed for are K, Ca, Ti, V, Cr, Mn, Fe, Co, Ni, Zn, As, Sr, Mo, Ba and Pb. All analyzed elements were evaluated for correlation with terrestrial age. The signal depth depends on the measured element and ranges from about 5 mm (Ba) to <1 mm for most elements (Zurfluh et al. 2011). Measurements were performed on exposed surfaces (ES), buried surfaces (BS) and cut surfaces (CS). Each measuring spot has a diameter of 8 mm. Since it is not possible to reconstruct the find situation of each meteorite, the more general term “natural surface” (NS) is used for unspecified external surfaces. On each surface at least three measurements were taken and the median values were taken for further calculations. The detection limit of Ba (around 100 µg/g) is relatively high. Initial Ba concentration of OC are between 3 to 5 µg/g (Wasson and Kallemeyn 1988). Small degrees of Ba contaminations are not detectable with HHXRF, therefore. The detection limit for V is also around 100 µg/g.

Other chemicals parameters that showed a correlation with terrestrial ages (Al-Kathiri et al. 2005), like H_2O or sulfur concentration, are not used in this study, since they cannot be analyzed by HHXRF and therefore are not suitable for the evaluation of large numbers of samples.

RESULTS

^{14}C terrestrial ages

In this work we use 128 ^{14}C terrestrial ages of meteorites. Fifty of them were reported by Al-Kathiri et al., (2005). Additional data were determined by Jull et al. (2008) and Giscard et al. (2009). 51 new terrestrial ages are reported in this paper (Table 3, a compilation of all used ^{14}C ages is given in Table S1). The 51 new ages comprise 8 LL, 17 L and 26 H chondrites. Overall, the ages range from <1 ka up to the limit of the ^{14}C method, 30 to 55 ka (Welten et al. 2004). The new ^{14}C age data are shown in Table 3. The mean age of the newly dated meteorites is 19.6 ka (median: 17.9 ka; st. dev.: 10.2 ka), which is congruent to the mean of the previous set, 21.5 ka (median 17.9 ka; st. dev.: 13.0 ka; Al-Kathiri et al., 2005). For all dated meteorites, the mean terrestrial age is 21.0 ka, the abundance maximum is 19.9 ka (median: 19.5 ka; st. dev.: 11.3 ka), whereas the percentage of samples of 0 to 10 ka is 19% and of samples >30 ka ~25%. The age distribution of all ^{14}C dated Omani ordinary chondrites (Fig. 4a) is characterized by a prominent lack of samples in the age range 0 to 10 ka, as previously observed based on a smaller dataset (Al-Kathiri et al. 2005).

Macroscopic weathering parameters and terrestrial age

Figure 5 shows the variation of ^{14}C terrestrial ages as a function of the intensity of macroscopic weathering parameters. There is a clear general increase of terrestrial ages with increasing intensity of the weathering for seven of the parameters (Fig. 5 a to g), only greenish staining due to Ni-serpentine precipitation on BS and calcite deposition on BS (Fig. 5 h, i) do not seem to be age correlated. Correlations (Table S2) of three macroscopic weathering parameters (salt on CS, fusion crust, sand attached on ES) are relatively high (R =

0.60 to 0.66) with the weathering degree, the same parameters also show elevated correlations with terrestrial age (R = 0.47 to 0.50). Correlations of macroscopic weathering parameters with chemical weathering parameters are only weak.

Weathering degree and terrestrial age

The weathering degree was determined for all ^{14}C dated ordinary chondrites from Oman using the refined scale (see methods). Plots of weathering degree versus ^{14}C terrestrial age (Fig. 6) show a clear increase of age with increasing weathering degree, but the variation of ages is quite large for single weathering degrees. We observe a positive correlation of the refined weathering scale with ^{14}C terrestrial age (R = 0.60), notably also for the newly defined stages W3.0 to W4.5 (Fig. 6). A plot of the median values of the ages for each weathering degree (Fig. 6b) shows that all three ordinary chondrite groups show comparable increases of terrestrial ages with increasing weathering degree, with correlations increasing from types H to LL (H: R=0.53, L: R=0.60 and LL: R=0.81). The weathering degree shows the best correlation of all investigated parameters with the terrestrial age.

Chemical parameters

From the meteorites collected in Oman, 368 meteorites were analyzed using handheld XRF (HHXRF). In total, the data of 5586 measurements were evaluated (Table S1). The most prominent contaminations are by Sr and Ba, consistent with the results of other studies on hot desert meteorites (e.g., Al-Kathiri et al. 2005; Crozaz et al. 2003; Nazarov et al. 2004b; Saunier et al. 2010; Shih et al. 2002; Stelzner et al. 1999). The highest concentrations on CS are 888 µg/g for Sr and 554 µg/g for Ba, respectively. On natural surfaces of the meteorites, contaminations are typically much higher. Profiles measured through cut slabs of several meteorites showed relatively constant concentrations in the interior and highly elevated concentrations either on one or both of the natural surfaces (ES or BS; Fig. 7). In most analyzed meteorites, the accumulation of Sr and Ba, as well as of Mn and V, elements typically associated with desert varnish (Dorn 2009; Engel and Sharp 1958), is similar on ES and BS. Maximum values detected on natural surfaces (comprising ES and/or BS) are ~3500 µg/g for Sr and ~650 µg/g for Ba. To test for correlations between elemental contaminations and terrestrial age, data from 98 ^{14}C dated chondrites (14 LL, 34 L and 50 H) were evaluated.

The resulting correlations of the chemical parameters with ^{14}C terrestrial ages are relatively weak when compared with correlations between weathering degree or macroscopic weathering parameters and ^{14}C terrestrial age (Table S2). For the elements with the best correlations (Ba_{ES}, Cr_{BS}, Fe_{CS}/Mn_{CS}, Mn_{ES}/Mn_{CS}, Sr_{CS}, Sr_{ES} and V_{BS}), median concentrations for different age steps are shown in Figure S1.

All other measured elements either show no significant variation caused by terrestrial alteration (K, Ca, Ti, Co, Ni), or concentrations are near to below limits of detection (Zn, As, Mo, Pb).

DISCUSSION

^{14}C terrestrial age distribution

The newly-obtained terrestrial ages (Table 3) confirm the previously observed (Al-Kathiri et al. 2005; Jull 2006) relative abundance of ^{14}C age groups observed in Oman. The mean ^{14}C age is 21.0 ka and there is a prominent lack of young (<10 ka) samples (Fig. 4). Since we have dated only a limited number of the found meteorites (corrected for pairing: 111 out of about 880 fall events or about 12%), two selected meteorite populations were used as a control: i) all samples found on petrified, fossil dunes of the western Ramlat al Wahibah, named RaW and ii) all LL samples. These two groups show a similar age pattern with a lack of young (<10 ka) and old (>40 ka) meteorites, even though those two populations are less representative due to the low number of samples (Fig. S2).

A similar terrestrial age (and weathering grade) distribution as in Oman was observed for a smaller OC population (n = 21) from the United Arab Emirates (UAE), found in the same geological environment as the meteorites from Oman (Hezel et al. 2011).

Considering all OC collected by our group since 2001 (corrected for pairing, not all reclassified for refined weathering degree), we still observe a dramatic lack of samples at low weathering grades (W≤2) or heavily weathered samples (only one W5 sample!). We believe this underabundance of young and old samples is present in the whole population. The same situation applies for the population of OC collected by other groups in Oman with independently determined weathering degrees (c.f. Meteoritical Society Database).

Only six of the analyzed meteorites showed no detectable ^{14}C. In general, few meteorites from the hot deserts of northern Africa, Arabia, Australia and north America show high terrestrial ages and no detectable ^{14}C, indicating that only rare samples survive longer than ~40 to 50 ka under the prevalent conditions. One OC with very high terrestrial age is known from the Dar al Gani area (DaG 343, H4 S2 W4), with a ^{41}Ca terrestrial age of 150 ± 40 ka, (Welten et al. 2004). Other meteorites from hot deserts with high terrestrial ages are lunar meteorite Dhofar 025 (0.5 – 0.6 Ma) and the shergottite Dhofar 019 (0.34 Ma, (Nishiizumi et al. 2002). On the other hand, OC populations from the Atacama desert in Chile appear to be dominated by meteorites with generally higher terrestrial ages (Gattacceca et al. 2011).

Meteorites of weathering degrees >4.5 might be missing due to the neutralization and passivation that occurs at W4.0 (Bland et al. 1998; Zurfluh et al. 2013). The cementation of pore space, washing out of salts and neutral to basic pH conditions after completion of troilite oxidation, slow chemical weathering processes. Physical weathering, most prominently wind ablation, dominates the late weathering history of OC from Oman.

Given a constant flux and age-dependent weathering, the age-abundance function should be decreasing with age, the youngest age group being the most abundant (Jull 2006). The observed under abundance of very young (<10 ka) OC is difficult to explain. Possible scenarios are: (i) selective removal by recent fast weathering of exposed young meteorites, while the old population is mostly buried; (ii) selective removal due to collection of unaltered meteorites by humans; (iii) selective burial of fresh falls in the soil; (iv) recent change of the meteorite flux; (v) a generally much higher age of the population combined with common contamination of old meteorites with ^{14}C, resulting in the ~20 ka abundance maximum. These scenarios are discussed in the following: (i) We see no evidence of unusually rapid erosion or weathering among the young meteorites. While the meteorite recovery areas of Oman experienced periods of more humid climatic conditions around 10 to 5 ka ago (Fleitmann and Matter 2009; Preusser 2009), the last 5 ka were dominated by relatively dry conditions. (ii) If humans had preferentially collected young meteorites (e.g., as source of iron), there should be evidence of such use in the archaeological collections of Oman, which is not the case (Hofmann et al. 2014). (iii) Freshly fallen meteorites of small to moderate size (tens to hundreds of grams), constituting the majority of the Oman desert meteorite population, typically are found on the surface of various types of soils and are not buried (e.g., Aoudjehane et al. 2012; Shaddad et al. 2010). (iv) Based on fireball observations and studies of old meteorite populations dated for terrestrial age, e.g., from Antarctica (Zolensky 1998), it is assumed that meteorite flux was constant over the period meteorites have accumulated in Oman (Bland et al. 1996; Halliday et al. 1989; Zolensky et al. 2006). In addition, if the flux was higher 15 to 20 ka ago, similar patterns had to be observed in other recovery areas, which is not the case. The meteorite population from western Australia has a higher percentage of young samples and shows an expected age distribution, i.e., decreasing abundances of samples with increasing terrestrial age (Jull et al. 2010). Also, meteorites from Algeria show an approximately exponential drop-off with increasing terrestrial age (Jull 2006). A similar situation, like that of Oman, is observed in the Roosevelt County, New Mexico, recovery areas, where a similar lack of young meteorites is observed (Jull 2006). There, meteorites are found in blowouts in the cover sands of late Quaternary age, which might explain the deficiency of younger meteorites (Zolensky et al. 1992). In Oman we observe that meteorites must have been buried in sand/soil for parts of their terrestrial residence as we frequently find meteorites with attached sand on buried as well as exposed surfaces (e.g., Fig. 1c). (v) Contamination with ^{14}C during terrestrial residence is possible, but care is taken by cleaning of samples before analysis by acid treatment and then heating in oxygen (Jull 2006). A high age of the population would be required, which is inconsistent with weathering rates observed in other hot desert areas. Also, the observed correlations between ^{14}C ages and weathering parameters would be difficult to explain.

Correlations of weathering parameters with ^{14}C terrestrial age and age estimation

The search for correlations between weathering parameters and terrestrial ages was motivated by the idea to find a set of chemical and/or physical parameters that would allow an independent estimation of the terrestrial age of meteorites. With ~880 different fall events represented in our collection of Omani meteorites, it appears impractical to obtain ^{14}C ages for all of them, while understanding the age distribution of the whole population is one of our goals. In general, the observed correlations (Table S2, Figs. 5, 6 and S1) are rather weak and there is considerable scatter in the data.

We have evaluated the correlation between the newly defined weathering degree and ^{14}C ages, as this parameter shows the best correlation (R=0.60) and is relatively easy to obtain. The ^{14}C age-weathering degree correlation clearly benefits from the refinement of the stages W3 into W3.0, W3.3 and W3.6 and W4 into W4.0 and W4.5. The eight weathering degrees observed (W0 to W4.5) only allow the assignment of eight ages. Based on the mean and standard deviation of ^{14}C ages of each weathering degree, the following ages are assigned: W0: 2±2 ka (arbitrary, only one sample), W1: 8.3±3.5 ka (n = 8), W2: 11.0±5.6 ka (n =20), W3.0: 14.5±6.3 ka (n = 23), W3.3: 17.4±6.1 ka (n = 15), W3.6: 23.2±10.2 ka (n = 13), W4.0: 27.9±9.1 ka (n = 39), W4.5: 32.5±9.9 ka (n = 9). Using the number of samples of each weathering degree and the above values only, we calculated a model age distribution with 5 ka bins (Fig. 8) by adding gaussian probability curves. The obtained probability distribution is very similar to the observed one. The mean deviation of calculated relative to observed numbers of samples in each 5 ka age bin is <10%, the correlation factor for measured versus modeled sample numbers per age bin is 0.97. The mean age calculated from the modeled distribution is 20.4 ka (mean of analyzed samples: 19.9 ka). We conclude that weathering degree-based age estimations can reliably be used for the calculation of age probability plots for whole meteorite populations. However, the error of age estimations for single samples is too large for a meaningful use in most applications.

Chemical weathering parameters

No single chemical parameter shows a good correlation with terrestrial age. This is likely due to the fact that concentrations of contaminating elements are heterogeneous on single samples, both on a natural surfaces (ES, BS, NS) and in the interior (cut surface, CS). In addition, contamination profiles (Fig. 7) are not linear and the degree of contamination likely is not strictly time dependent since it is affected by a number of factors including porosity, which is variable initially and is subject to repeated changes during weathering history (Bland et al. 1998; Britt and Consolmagno 2003; Consolmagno et al. 2008; Macke et al. 2010; Zurfluh et al. 2013). Another factor influencing elemental contamination is wind erosion. Thin coatings (desert varnish like) of contaminants on natural surfaces are continuously eroded by sand blasting. Wind ablation is a strong physical weathering process and is observed on nearly all (older) meteorites from Oman. Superficial concentrations of Sr, Ba and V are highly variable. The best correlations with ^{14}C terrestrial age among the chemical weathering parameters are shown by the ratio of Mn_{ES} relative to Mn_{CS} and by Fe_{CS}/Mn_{CS}, Table S2). The higher Mn_{ES}/Mn_{CS} ratios for older meteorites indicate Mn accumulation due to desert varnish formation. In an approach similar to ours, the possible use for age dating of Mn-accumulations quantified using by HHXRF on varnished rock surfaces with petroglyphs has been evaluated by various authors with limited success (Lytle 2009; Lytle et al. 2000; Pingitore and Lytle 2003; Pingitore et al. 2004).

The age dependent variations of Fe/Mn ratios on CS likely are a result of the analytical method (HHXRF). The presence of Fe metal grains in a silicate matrix results in an underestimation of bulk Fe due to high self absorption of X-rays in Fe metal. To minimize these effects, the instrument was calibrated using powders and hand specimens (Zurfluh et al. 2011). During weathering, iron is partially redistributed resulting in a bulk sample with more homogeneous absorption coefficients. The Fe/Mn ratio determined by HHXRF indirectly determines the oxidation degree, therefore. The effect was observed in all groups, even in metal-poor LL chondrites.

CONCLUSIONS

Several macroscopic, microscopic, and chemical weathering parameters observed in ordinary chondrites from Oman show a correlation with the ^{14}C terrestrial age of the respective meteorites, but the correlations are generally rather weak, especially in the case of chemical parameters. The best correlation is obtained using a refined weathering degree scale defined in this work, which is based on and refines the Wlotzka (1993) scale. We demonstrate that the terrestrial age distribution as observed among 128 ^{14}C dated meteorites could be reconstructed as age probability diagrams using weathering degree and mean ^{14}C ages of the age groups. This offers the possibility to determine age distributions for the whole Oman meteorite collection, once the refined weathering degrees are determined for all samples. The ^{14}C terrestrial age distribution of ordinary chondrites from Oman, characterized by an abundance maximum at 19.9 ka and a lack of young (0 to 10 ka) samples remains poorly understood and requires further research.

Acknowledgments

We thank Ali Al Rajhi, Salim Al-Busaidi and Hilal Al Azri, from the Public Authority for Mining (formerly Directorate General of Minerals), Ministry of Commerce and Industry, Muscat, for the permission to perform searches in Oman, work on the samples and for companionship in the field. Marc Dupayrat, Roland Bächli and Björn Klaue are acknowledged for their help with the Niton HHXRF instrument. The effort of Tom Burri during macroscopic weathering classification and his input into the discussion of the classification criterions are appreciated. Constructive comments by Kees Welten, Ingo Leya and anonymous reviewers on earlier versions of the manuscript improved the paper. This work was supported by Swiss National Science Foundation (grants 119937 and 137924).

REFERENCES

Al-Kathiri, A., Hofmann, B. A., Jull, A. J. T., and Gnos, E. 2005. Weathering of meteorites from Oman: Correlation of chemical and mineralogical weathering proxies with ^{14}C terrestrial ages and the influence of soil chemistry. *Meteoritics & Planetary Science* 40:1215-1239.

Aoudjehane, H. C., Avice, G., Barrat, J. A., Boudouma, O., Chen, G., Duke, M. J. M., Franchi, I. A., Gattacceca, J., Grady, M. M., Greenwood, R. C., Herd, C. D. K., Hewins, R., Jambon, A., Marty, B., Rochette, P., Smith, C. L., Sautter, V., Verchovsky, A., Weber, P., and Zanda, B. 2012. Tissint Martian Meteorite: A Fresh Look at the Interior, Surface, and Atmosphere of Mars. *Science* 338:785-788.

Bevan, A. W. R., Downes, P. J., and Thompson, M. 2001. Little Minnie Creek, a L4(S2) ordinary chondritic meteorite from Western Australia. *Journal of the Royal Society of Western Australia* 84:149-152.

Bland, P. A. 2006. Terrestrial weathering rates defined by extraterrestrial materials. *Journal of Geochemical Exploration* 88:257-261.

Bland, P. A., Berry, F. J., Smith, T. B., Skinner, S. J., and Pillinger, C. T. 1996. The flux of meteorites to the Earth and weathering in hot desert ordinary chondrite finds. *Geochimica et Cosmochimica Acta* 60:2053-2059.

Bland, P. A., Sexton, A. S., Jull, A. J. T., Bevan, A. W. R., Berry, F. J., Thornley, D. M., Astin, T. R., Britt, D. T., and Pillinger, C. T. 1998. Climate and rock weathering: A study of terrestrial age dated ordinary chondritic meteorites from hot desert regions. *Geochimica et Cosmochimica Acta* 62:3169-3184.

Britt, D. T. and Consolmagno, G. J. 2003. Stony meteorite porosities and densities: A review of the data through 2001. *Meteoritics & Planetary Science* 38:1161-1180.

Cassidy, W. A. 1980. Discovery of the Allan Hills A77, Antarctica, meteorites. In: Graham, A. L. (Ed.), *The Meteoritical Bulletin No. 57*. The meteoritical society.

Consolmagno, G. J., Britt, D. T., and Macke, R. J. 2008. The significance of meteorite density and porosity. *Chemie der Erde-Geochemistry* 68:1-29.

Crozaz, G., Floss, C., and Wadhwa, M. 2003. Chemical alteration and REE mobilization in meteorites from hot and cold deserts. *Geochimica et Cosmochimica Acta* 67:4727-4741.

Dorn, R. I. 2009. The rock varnish revolution: New insights from microlaminations and the contributions of Tanzhuo Liu. *Geography Compass* 3:1-20.

Engel, C. G. and Sharp, R. P. 1958. Chemical data on desert varnish. *Geological Society of America Bulletin* 69:487-&.

Fleitmann, D. and Matter, A. 2009. The speleothem record of climate variability in Southern Arabia. *Comptes Rendus Geoscience* 341:633-642.

Gattacceca, J., Valenzuela, M., Uehara, M., Jull, A. J. T., Giscard, M., Rochette, P., Braucher, R., Suavet, C., Gounelle, M., Morata, D., Munayco, P., Bourot-Denise, M., Bourles, D., and Demory, F. 2011. The densest meteorite collection area in hot deserts: The San Juan meteorite field (Atacama Desert, Chile). *Meteoritics & Planetary Science* 46:1276-1287.

Gibson, E. K., Jr. and Bogard, D. D. 1978. Chemical alterations of the Holbrook chondrite resulting from terrestrial weathering. *Meteoritics* 13.

Giscard, M. D., Jull, A. J. T., and Hewitt, L. R. 2009. Terrestrial carbonates of meteorites from Chile, Oman, Northwest Africa and Saudi Arabia. *Meteoritics & Planetary Science* 44:A78-A78.

Goddard, E. N., Trask, P. D:, De Ford, R. K., Rove, O. N., Singewald, J. T., Jr., and Overbeck, R. M. 1948. Rock-color chart. Boulder, Colorado. *Geological Society of America.* :11 p.

Gooding, J. L. 1986. Weathering of stony meteorites in Antarctica. *International Workshop on Antarctic Meteorites,*

Gooding, J. L. 1989. Significance of terrestrial weathering effects in Antarctic meteorites. In: Marvin, U. B. and MacPhearson, G. J. Eds., *Field and Laboratory Investigations of Meteorites from Victoriay Land and the Thiel Mountains Region, Antarctica, 1982-1983 and 1983-1984*. Smithsonian Contrib. Earth Sci.

Halliday, I., Blackwell, A. T., and Griffin, A. A. 1989. The flux of meteorites on the Earth's surface. *Meteoritics* 24:173-178.

Hezel, D. C., Schlüter, J., Kallweit, H., Jull, A. J. T., Al-Fakeer, O. Y., Al-Shamsi, M., and Strekopytov, S. 2011. Meteorites form the United Arab Emirates: Description, weathering, and terrestrial ages. *Meteoritics & Planetary Science* 46:327-336.

Hofmann, B. A., Gnos, E., and Al-Kathiri, A. 2004. Harvesting meteorites in the Omani desert: Implications for astrobiology. *Proceedings of the Third European Workshop on Exo-Astrobiology,*

Hofmann, B. A., Gnos, E., Greber, N. D., Federspiel, N., Burri, T., Zurfluh, F. J., Al-Battashi, M., and Al-Rajhi, A. 2014. The Omani-Swiss Meteorite Search Project: Update And The Quest For Missing Irons. *Meteoritics & Planetary Science* 49:A170-A170.

Huber, L., Gnos, E., Hofmann, B., Welten, K. C., Nishiizumi, K., Caffee, M. W., Hillegonds, D. J., and Leya, I. 2008. The complex exposure history of the Jiddat al Harasis 073 L-chondrite shower. *Meteoritics & Planetary Science* 43:1691-1708.

Ikeda, Y. and Kojima, H. 1991. Terrestrial alteration of Fe-Ni metals in Antarctic ordinary chondrites and the relationship to their terrestrial ages. *Praoc. NIPR Symp. Antarct. Meteorites* 4:307-318.

Jull, A. J. T. 2006. Terrestrial ages of meteorites. In: Lauretta, D. S. and McSween, H. Y. Eds., *Meteorites and the Early Solar System II*. University of Arizona Press, Tucson.

Jull, A. J. T., Cloudt, S., and Cielaszyk, E. 1998. ^{14}C terrestrial ages of meteorites from Victoria Land, Antarctica, and the infall rate of meteorites. In: McCall, G. J., Hutschison R., Grady, M. M., and Rothery, D. Eds., *Meteorites: Flux with time and impact effects*. Geological Society of London Special Publication #140, London.

Jull, A. J. T., Donahue, D. J., Cielaszyk, E., and Wlotzka, F. 1993. Carbon-14 terrestrial ages and weathering of 27 meteorites from the southern high-plains and adjacent areas (USA). *Meteoritics* 28:188-195.

Jull, A. J. T., Donahue, D. J., and Linick, T. W. 1989. Carbon-14 activities in recently fallen meteorites and Antarctic meteorites. *Geochimica et Cosmochimica Acta* 53:2095-2100.

Jull, A. J. T., Leclerc, M. D., Biddulph, D. L., McHargue, L. R., Burr, G. S., Al-Kathiri, A., Gnos, E., and Hofmann, B. 2008. Radionuclide studies of meteorites from Ramlat al Wahibah and other Omani desert locations. *Meteoritics & Planetary Science* 43:A69-A69.

Jull, A. J. T., McHargue, L. R., Bland, P. A., Greenwood, R. C., Bevan, A. W. R., Kim, K. J., LaMotta, S. E., and Johnson, J. A. 2010. Terrestrial ages of meteorites from the Nullarbor region, Australia, based on ^{14}C and ^{14}C-^{10}Be measurements. *Meteoritics & Planetary Science* 45:1271-1283.

Jull, A. J. T., Wlotzka, F., and Donahue, D. J. 1991. Terrestrial ages and petrologic description of Roosevelt County meteorites *Lunar and Planetary Science XXII,,*

Jull, A. J. T., Wlotzka, F., Palme, H., and Donahue, D. J. 1990. Distribution of terrestrial age and petrologic type of meteorites from western Libya. *Geochimica et Cosmochimica Acta* 54:2895-2898.

Lee, M. R. and Bland, P. A. 2004. Mechanisms of weathering of meteorites recovered from hot and cold deserts and the formation of phyllosilicates. *Geochimica et Cosmochimica Acta* 68:893-916.

Losiak, A. and Velbel, M. A. 2011. Evaporite formation during weathering of Antarctic meteorites--A weathering census analysis based on the ANSMET database. *Meteoritics & Planetary Science* 46:443-458.

Lytle, F. 2009. How old are petroglyphs? Prove it. *Nevada Rock Art Foundation meeting, Mesquite NV.*

Lytle, F. W., Pingitore, N. E., Lytle, N. W., Ferris-Rowley, D., and Reheis, M. C. 2000. Determination of growth rate of desert varnish: Application to dating petroglyphs. *Workshop on Synchrotron Radiation in Art and Archaeology, SSRL.*

Macke, R. J., Consolmagno, G. J., Britt, D. T., and Hutson, M. L. 2010. Enstatite chondrite density, magnetic susceptibility, and porosity. *Meteoritics & Planetary Science* 45:1513-1526.

Nazarov, M. A., Badyukov, D. D., Lorents, K. A., and Demidova, S. I. 2004a. The flux of lunar meteorites onto the Earth. *Solar System Research* 38:49-58.

Nazarov, M. A., Demidova, S. I., Patchen, A., and Taylor, L. A. 2004b. Dhofar 311, 730 and 731: new lunar meteorites from Oman. *Lunar and Planetary Science XXXV, Abstract #1233,*

Nishiizumi, K., Okazaki, R., Park, J., Nagao, K., Masarik, J., and Finkel, R. 2002. Exposure and terrestrial history of Dhofar 019 Martian meteorite (abstract #1366). *33rd Lunar and Planetary Science Conference,*

Pingitore, N. E. and Lytle, F. W. 2003. Desert varnish: Relative and absolute dating using portable X-ray fluorescence. *EOS Trans. AGU* 84.

Pingitore, N. E., Lytle, F. W., Rowley, P. D., and Ferris, D. E. 2004. Absolute dating of desert varnish using portable X-ray fluorescence: Calibration and testing. *American Geophysical Union, Fall Meeting 2004*:abstrct #B33B-0266.

Preusser, F. 2009. Chronology of the impact of Quaternary climate change on continental environments in the Arabian Peninsula. *Comptes Rendus Geoscience* 341:621-632.

Preusser, F., Radies, D., and Matter, A. 2002. A 160'000-year record of dune development and atmospheric circulation in southern Arabia. *Science* 296:2018-2020.

Radies, D., Preusser, F., Matter, A., and Mange, M. 2004. Eustatic and climatic controls on the development of the Wahiba Sand Sea, Sultanate of Oman. *Sedimentology* 51:1359-1385.

Ruzicka, A. 1995. Nullarbor-018 - A new L6 chondrite from Australia. *Meteoritics* 30:102-105.

Saunier, G., Poitrasson, F., Moine, B., Gregoire, M., and Seddiki, A. 2010. Effect of hot desert weathering on the bulk-rock iron isotope composition of L6 and H5 ordinary chondrites. *Meteoritics & Planetary Science* 45:195-209.

Shaddad, M. H., Jenniskens, P., Numan, D., Kudoda, A. M., Elsir, S., Riyad, I. F., Ali, A. E., Alameen, M., Alameen, N. M., Eid, O., Osman, A. T., AbuBaker, M. I., Yousif, M., Chesley, S. R., Chodas, P. W., Albers, J., Edwards, W. N., Brown, P. G., Kuiper, J., and Friedrich, J. M. 2010. The recovery of asteroid 2008 TC3. *Meteoritics & Planetary Science* 45:1557-1589.

Shih, C.-Y., Nyquist, L. E., Reese, Y., Wiesmann, H., Nazarov, M. A., and Taylor, L. A. 2002. The choronology and petrogenesis of the mare basalt clast from lunar meteorite Dhofar 287: Rb-Sr and Sm-Nd isotopic studies. *Lunar and Planetary Science XXXIII, Abstract #1344,*

Stelzner, T., Heide, K., Bischoff, A., Weber, D., Scherer, P., Schultz, L., Happel, M., Schron, W., Neupert, U., Michel, R., Clayton, R. N., Mayeda, T. K., Bonani, G., Haidas, I., Ivy-Ochs, S., and Suter, M. 1999. An interdisciplinary study of weathering effects in ordinary chondrites from the Acfer region, Algeria. *Meteoritics & Planetary Science* 34:787-794.

Velbel, M. A. 1988. The distribution and significance of evaporitic weathering products on Antarctic meteorites. *Meteoritics* 23:151-159.

Wasson, J. T. and Kallemeyn, G. W. 1988. Compositions of chondrites. *Philosophical Transactions of the Royal Society of London Series a-Mathematical Physical and Engineering Sciences* 325:535-544.

Welten, K. C., Nishiszumi, K., Finkel, R. C., Hillegonds, D. J., Jull, A. J. T., Franke, L., and Schultz, L. 2004. Exposure history and terrestrial ages of ordinary chondrites from the Dar al Gani region, Libya. *Meteoritics & Planetary Science* 39:481-498.

Wlotzka, F. 1993. A weathering scale for the ordinary chondrites. *Meteoritics* 28:460.

Zolensky, M. E. 1998. The flux of meteorites to Antarctica. In: McCall, G. J., Hutschison R., Grady, M. M., and Rothery, D. Eds., *Meteorites: Flux with time and impact effects*. Geological Society of London Special Publication #140, London.

Zolensky, M. E., Bland, P. A., Brown, P., and Halliday, I. 2006. Flux of extraterrestrial materials In: Lauretta, D. S. and McSween, H. Y. Eds., *Meteorites and the Early Solar System II*. University of Arizona Press, Tucson.

Zolensky, M. E., Rendell, H. M., Wilson, I., and Wells, G. L. 1992. The age of the meteorite recovery surfaces of Roosvelt County, New Mexico, USA. *Meteoritics* 27:460-462.

Zurfluh, F. J., Hofmann, B. A., Gnos, E., and Eggenberger, U. 2011. Evaluation of the utility of handheld XRF in meteoritics. *X-Ray Spectrometry* 40:449-463.

Zurfluh, F. J., Hofmann, B. A., Gnos, E., and Eggenberger, U. 2013. "Sweating meteorites"-Water-soluble salts and temperature variation in ordinary chondrites and soil from the hot desert of Oman. *Meteorit. Planet. Sci.* 48:1958-1980.

Tables

Table 1. Macroscopic weathering parameters

Intensity Code	Abbreviation	N = 0	N = 1	N = 2	N = 3
Wind ablation on [ES]	$Wind_{ES}$	No wind ablation visible	FC/rock surface with cavities/mild wind-polishing	"Monadnocks"/strong polishing	Ventifact, striation visible
Sand on [ES]	$Sand_{ES}$	No attached sand*	Some isolated sand grains attached	Abundant sand-grain-aggregates attached	No attached sand#
Fusion crust (FC) on [ES]	FC_{ES}	FC preserved [>80%]	FC partly eroded [20-80%]	Some FC remnants [2-20%]	No FC [<2%] preserved
Salt on [CS]	$Salt_{CS}$	No salts or hygroscopic behavior visible*	Few isolated droplets of hygroscopic salts	Extreme salt efflorescence / hygroscopic behavior	No salt or hygroscopic behavior visible#
Pore space on [CS]	$Pore_{CS}$	No macroscopic pore space	Empty pores	Pore space partially filled	All pore space filled
Cracks [ES]	$Crack_{ES}$	No cracks	Only few, narrow cracks	Several (wide) cracks, meteorite at most broken into a few pieces (usually <10).	Abundant wide cracks, whole meteorite broken into many pieces.
White precipitations [BS]	CC_{BS}	No white precipitation on buried surface	Isolated spots, white precipitation inside cracks	White precipitations spread mainly along and from cracks	Abundant white precipitation. >25% of [BS]. All cracks have precipitation of white minerals. White precipitations are also strongly present at the border of [ES] to [BS].
Green [BS]	$Green_{BS}$	No green Ni-rich minerals present on buried surface of the meteorite	A few isolated greenish spots within cracks are present. Mostly associated with terrestrial sand grains an iron hydroxides	Greenish minerals are abundant along cracks	Greenish staining occurs widely on the buried surface: along cracks , on the border of [ES] to [BS] and on spots with attached sand as well as iron hydroxide bloomings

Lichen on [ES]	Lichen$_{ES}$	No lichen	A few isolated lichens are present; <20% coverage of meteorite	Area wide lichen covers the meteorite, 20-80%	Full coverage meteorite by lichen, >80%
Red [BS]	Red$_{BS}$	Same as on [ES]	Small area of BS has slightly reddish color	Abundant red, >10% of [BS]	Bright rusty/red, >75% of [BS]

CS: cut surface

BS: buried surface

ES: exposed surface

* $N(FC) \geq 1$, $N(Wind) \leq 1$, $N(Red) \leq 1$ and if macroscopically fresh metal is visible on CS ($W \leq 2.0$)

$N(FC) \leq 1$, $N(Wind) \geq 1$ and when macroscopically no metal flakes are visible on CS ($W \geq 3.6$)

Table 2. The refined weathering degree classification

Weathering degree	Metal oxidation [vol%]	Troilite oxidation [vol%]	Comments
W0.0	0	0	Fresh, some iron-hydroxide staining possible
W1.0	<20	≥0	Minor oxide rims around metal and troilite, small iron oxides and iron hydroxide veins might be already present
W2.0	20-60	<20	Onset of veining with iron oxides and iron hydroxides
W3.0	>60	<20	Strong oxidation of metal, troilite shows only minor alteration
W3.3	>60	20-60	Strong oxidation of metal, troilite moderately altered. Usually a few troilites are completely oxidized
W3.6	>60[§]	>60[§]	Strong oxidation of metal and troilite. Most troilites are oxidized or show reduced reflectivity.
W4.0	>95	>95	Nearly complete oxidation of metal and troilite, usually some troilite remnants are visible
W4.5	100	100	All metal and troilite oxidized, only minor remnants of metal and troilite as inclusions in silicates; some silicate alteration (mainly olivine) possible
W5.0*	100	100	Metal and troilite 100% oxidized, major alteration of silicates, mainly olivine.
W6.0[#]	100	100	Massive replacement of silicates by clay and oxides

[§] When metal and troilite each are oxidized >95vol% the sample is classified as W4.0, while a sample with 100 vol% metal alteration and 90 vol% troilite alteration is still a W3.6.

* Since we have only one W5.0 sample in our collection, the definition of this step is still vague.

[#] W6.0 if fully adopted from Wlotzka (1993) since we have no such sample in our collection.

Classification guide:

The thin section should be prepared from a representative part of the interior of the sample. If several stages are visible take the mean.

Troilite and metal inclusions in shock veins, shock melts or other protecting materials should be excluded for classification.

Table 3. Classification and new terrestrial ages of OC from Oman.

Name	Class	P	S	W	^{14}C [dpm kg^{-1}]			TA [ka]		
Al Huqf 063	L	6	S2	3.6	3.0	±	0.8	23.4	±	2.6
Al Huqf 065	L	6	S5	2.0	49.4	±	2.0	0.3	±	1.3
Al Huqf 069	H	4/5	S2	3.0	0.7	±	0.3	34.3	±	3.5
JaH 343	LL	6	S3	1.0	24.5	±	1.0	6.7	±	1.3
JaH 413	H	4	S1	3.0	10.1	±	1.0	12.6	±	1.5
JaH 416	L	6	S5	4.0	2.9	±	0.8	23.8	±	2.7
JaH 418	H	4	S3	3.6	1.9	±	1.0	26.2	±	4.5
JaH 423	H	4	S3	3.3	5.3	±	0.6	18.0	±	1.6
JaH 474	LL	3.7-6	S2	3.0	27.7	±	1.1	5.7	±	1.3
JaH 493	L	6	S3-4	3.3	2.5	±	0.8	25.0	±	3.1
JaH 498	L	6	S4	3.6	1.7	±	0.8	28.3	±	4.0
JaH 578	H	6	S2	1.0	10.1	±	0.4	12.6	±	1.3
JaH 579	L	4-6	S3-5	3.3	16.0	±	0.4	9.6	±	1.3
JaH 620	L	6	S4	2.0	14.7	±	0.7	10.3	±	1.4
QaM 001	LL	4-6	S2	3.0	25.6	±	0.6	6.3	±	1.3
RaS 242	LL	4	S3	3.0	2.8	±	0.6	24.5	±	2.3
RaS 262	LL	6	S3	1.0	25.6	±	0.9	6.4	±	1.3
RaS 267	LL	6	S1	4.0	1.4	±	0.7	30.5	±	4.4
RaS 281	H	3-6	S2	3.0	5.3	±	0.3	17.9	±	1.4
RaS 290	L	6	S4	3.3	5.4	±	0.4	18.5	±	1.4
RaS 292	L	6	S2	3.0	14.1	±	0.3	9.8	±	1.3
RaS 295	H	4	S2	3.0	18.6	±	1.0	7.5	±	1.4
RaS 297	L	6	S4	4.5	2.2	±	0.3	25.9	±	1.7
RaS 302	H	4	S2	3.6	0.7	±	0.4	35.0	±	5.7
RaS 304	H	6	S2	3.3	6.2	±	0.4	16.2	±	1.4
RaS 316	L	5	S3	4.5	6.5	±	0.3	17.1	±	1.4
RaS 322	H	3	S1	3.0	13.7	±	0.3	10.1	±	1.3
RaW 002	H	4/5	S2	2.0	8.1	±	0.9	14.4	±	1.6
RaW 005	H	5	S3	4.0	0.7	±	1.2	34.2	±	13.1
RaW 007	H	5	S2	4.0	2.0	±	0.8	25.9	±	3.5
RaW 008	L	4	S2	3.0	2.3	±	0.8	25.5	±	3.2
RaW 010	H	4	S2-3	4.0	2.3	±	1.2	25.0	±	4.4
RaW 014	H	5	S2	2.0	20.2	±	0.9	6.9	±	1.3
RaW 015	H	5	S3	3.0	9.1	±	0.8	13.4	±	1.5
RaW 016	L	6	S4-5	4.5	1.0	±	0.6	32.5	±	5.4
RaW 017	H	5	S2	3.0	19.6	±	1.1	7.1	±	1.4
RaW 019	H	6	S1	4.5	0.9	±	0.8	32.2	±	7.1
RaW 021	H	5	S1	4.0	1.4	±	1.1	28.9	±	6.4
RaW 024	H	5	S2	1.0	32.7	±	1.2	2.9	±	1.3
RaW 027	H	5	S2-3	4.5	0.5	±	0.9	37.0	±	13.5
RaW 031	H	4	S2	3.0	3.3	±	0.9	22.0	±	2.7
RaW 034	LL	3-5	S2	0.0	23.9	±	1.0	6.9	±	1.3
RaW 035	H	5	S2	3.6	2.3	±	0.9	24.9	±	3.4
RaW 032	L	6	S4	4.5	<0.5			>38		
RaW 038	H	5	S2	4.5	<0.5			>38		
SaU 420	LL	6	S2	3.3	12.2	±	0.9	12.5	±	1.4
SaU 523	L	6	S4	3.3	6.5	±	1.1	17.0	±	1.9
Shalim 008	H	5	S3	2.0	5.8	±	0.3	17.2	±	1.4

UaS 009	L	6	S4	4.0	0.9	±	0.4	33.3	±	3.6
UaS 011	H	4	S1	3.0	3.1	±	0.4	22.4	±	1.6
UaS 013	L	6	S4	2.0	7.8	±	0.3	15.6	±	1.3

P: Petrologic type
S: Shock level
W: Weathering degree
TA: Terrestrial age
n.a.: not available

Figures

Fig. 1. Macroscopically visible weathering parameters. a) RaS 381, L6 S3 W3.3, shows prominent wind erosion on the exposed surface (ES). The buried part (BS) has still some remnants of fusion crust (FC). b) The cut surface (CS) of JaH 100, H4-5 S1 W3.0, shows efflorescences due to contamination with hygroscopic salts. Salt efflorescence also occurs on the exposed surface (ES) and some sand grains are attached due to precipitation of iron hydroxides on ES. The buried surface (BS) has attached caliche. c) Meteorite RaS 401, L3.8 S2 W3.3, recovered near dunes displays patches of attached sand. Empty pores are visible on cut surface (CS). d) The buried part of RaS 284, LL5 S1 W3.3, has a slightly reddish color and is distinct in color to that of ES.

Fig. 2. Weathering classification based on degree of oxidation of iron and troilite. a) Interpretation of the Wlotzka (1993) weathering grade classification. Metal oxidation of 20-60% defines W2. W3 and "W4" are subject to interpretation; the combined area considers the most logical. "W4" is interpreted to be >95% alteration of each metal and troilite individually. b) Our refined classification of weathering degrees divides W3 into three intermediate steps based on the degree of oxidation of troilite (W3.0, W3.3 and W3.6) The dashed lines indicate possible further subdivisions for W1.X and W2.X (not realized in our samples). Plotted data are for ordinary chondrite samples from Oman indicating typical weathering paths (Al-Kathiri et al. 2005).

Fig. 3. Reflected light photomicrographs of OCs from Oman showing typical examples of different weathering degrees. Note the continuous alteration of Fe-Ni-metal (white) and yellowish troilite to grey iron oxides and iron hydroxides and the increasing veining with iron (oxi)hydroxides. Scale bar at bottom right is 200 μm. a) SaU 424, L6 S3 W0.0 b) JaH 578, H6 S2 W1.0 c) RaS 311 H4-6 S3 W2.0 d) Al Huqf 069, H4/5 S2 W3.0 e) RaS 304, H6 S2 W3.3 f) RaS 114, H5 S1/2 W3.6 g) RaW 022, H5 S3 W4.0 h) RaW 041, H6 S1 W4.5

Fig. 4. Histograms of a) ^{14}C terrestrial ages and of b) weathering degrees.

Fig. 5. Terrestrial ages of OCs as a function of macroscopically visible weathering parameters showing median values, 50 percentile boxes and full range of data.

Fig. 6. Relation between terrestrial ages and weathering degrees of OC from Oman. a) All data, showing a general increase, with a lot of scatter, of ^{14}C ages with increasing weathering degree. b) Median terrestrial ages for individual weathering degrees. No significant difference between H, L and LL chondrites are discernible. Note the systematic increase of terrestrial ages among the newly defined weathering subgroups W3.0-W4.5.

Fig. 7. Profiles of Sr and Mn concentrations on exposed/cut/buried surfaces of OC measured with HHXRF. Distance 0 indicates a spot measured on the exposed surface. The lowermost point was obtained on the buried surface. The shaded area indicates the part of the meteorite originally buried in the soil. a) JaH 468, L6 S3 W2.0, shows Sr enrichment on ES and BS. b)

Meteorite RaS 340, L6 S4 W4.0, shows dominant Sr enrichment on ES. c) RaS 341, L6 S1 W1.0, shows dominant Sr contamination in its lower part. d) A sample from the JaH 091 strewn field (L5 S2), shows Mn enrichments both on ES and BS.

Fig. 8. Modeling of the age-frequency distribution with 5 ka age bins. Filled circles show the ^{14}C age distribution of all analyzed OC's. Empty squares show the age distribution calculated from weathering degrees (see text) for the same group of 128 OC's.

Supplementary information:

Fig. S1. Data used for age estimations with chemical parameters. The plots a), c), e), g), i) and k) are data as analyzed by HHXRF. Each data point represents the median of at least three measurements. At right, the median element concentrations of 5 ka age steps of all OC groups are displayed in b), d), f), h), j) and l).

Fig. S2. Age distribution of a) all Ramlat al Wahiba (RaW) meteorites and b) all LL chondrites found during our searches in Oman.

Table S1. Raw data, compilation of meteorite classification, chemical and macroscopic parameters, terrestrial ages

Table S2. Correlation matrix

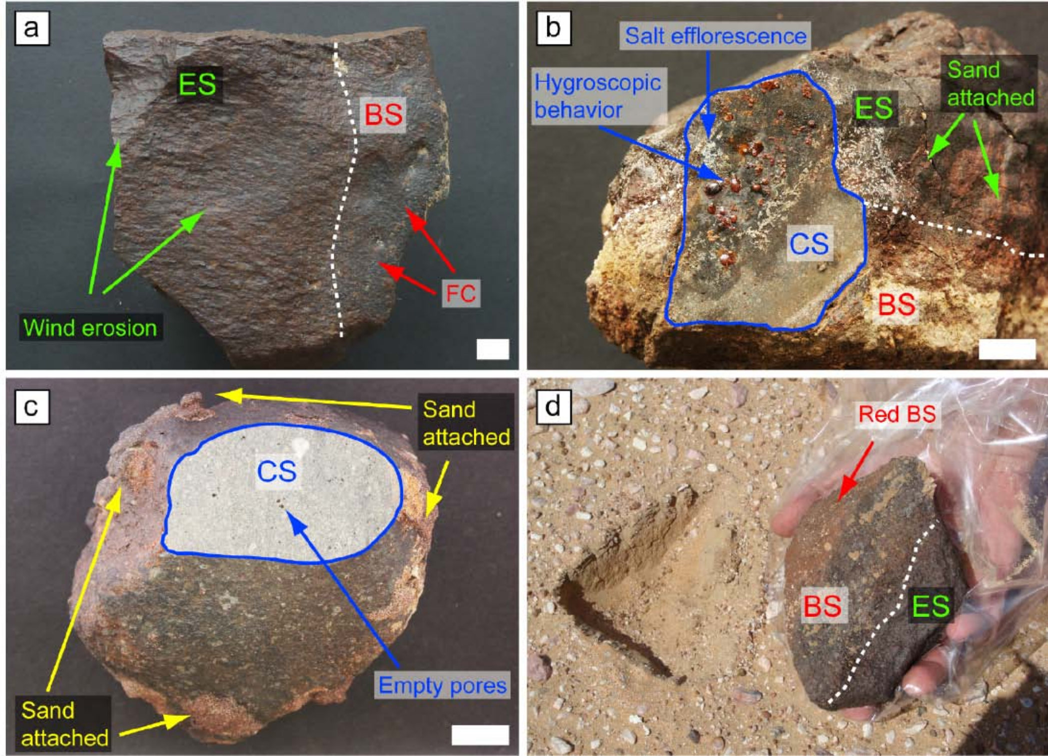
a
ES
BS
FC
Wind erosion
b
Salt efflorescence
Hygroscopic behavior
Sand attached
ES
CS
BS
c
Sand attached
CS
Empty pores
Sand attached
d
Red BS
BS
ES

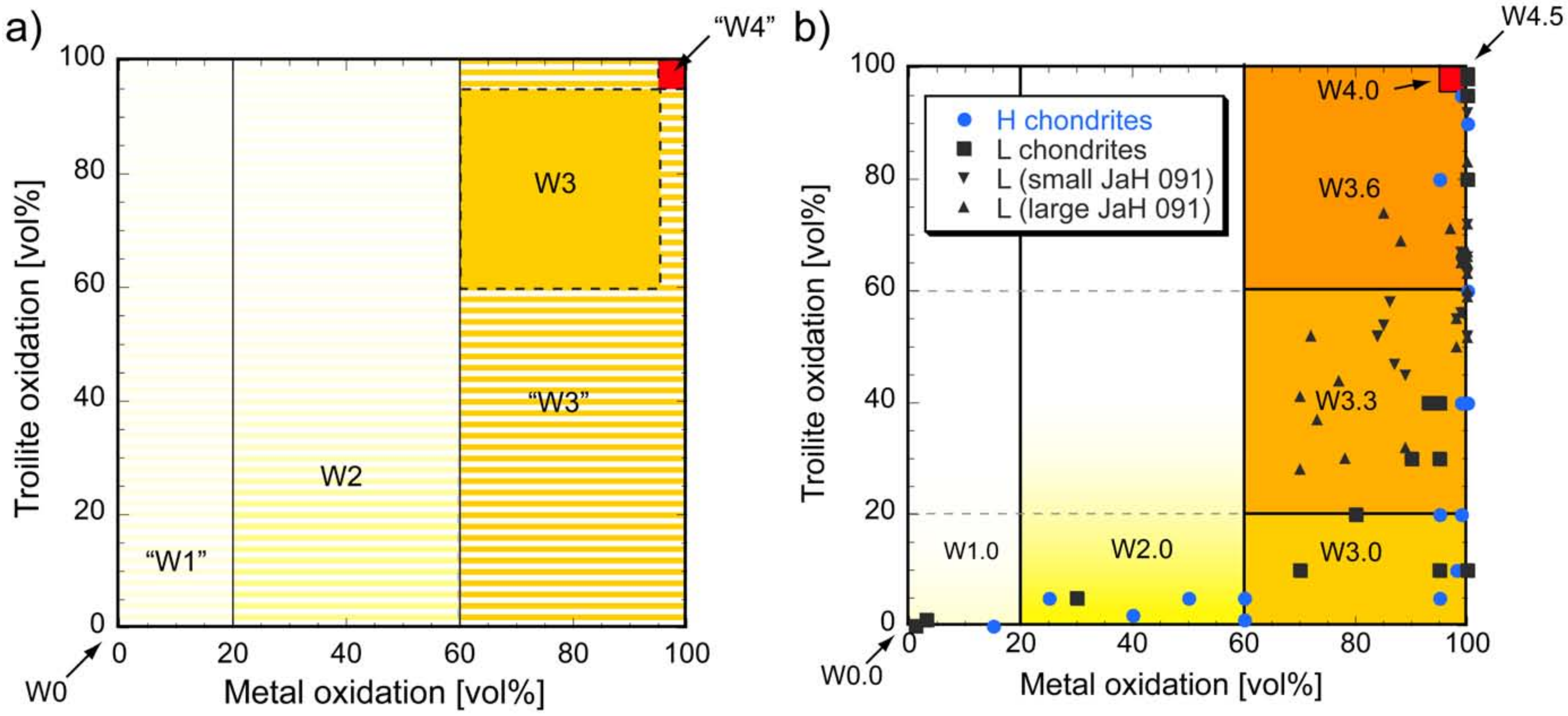

a)
"W4"
100
80
60
40
20
0
W3
"W3"
W2
"W1"
W0
0
20
40
60
80
100
Troilite oxidation [vol%]
Metal oxidation [vol%]
b)
W4.5
W4.0
H chondrites
L chondrites
L (small JaH 091)
L (large JaH 091)
W3.6
W3.3
W3.0
W2.0
W1.0
W0.0
Troilite oxidation [vol%]
Metal oxidation [vol%]

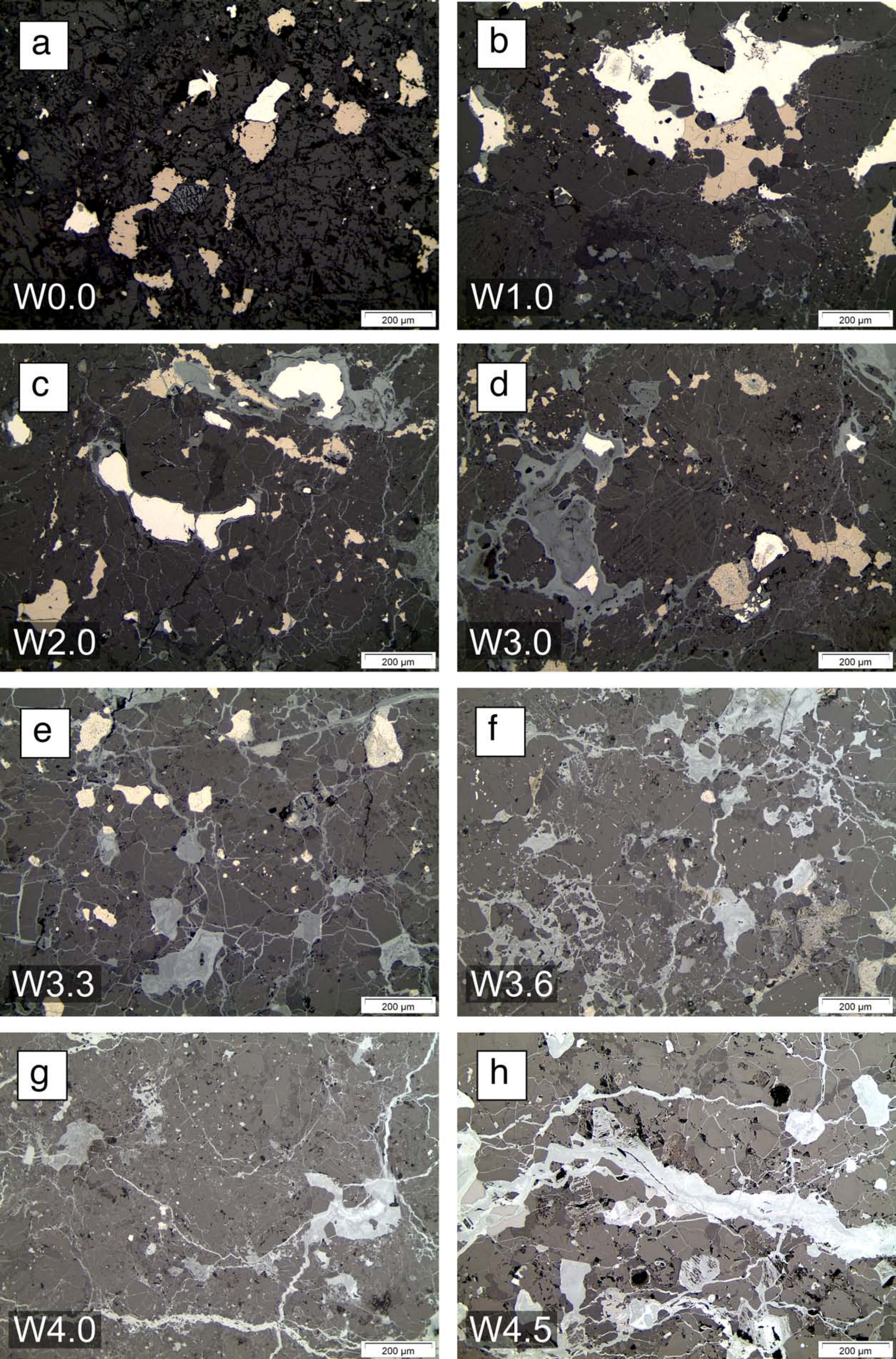
a
W0.0
200 μm
b
W1.0
200 μm
c
W2.0
200 μm
d
W3.0
200 μm
e
W3.3
200 μm
f
W3.6
200 μm
g
W4.0
200 μm
h
W4.5
200 μm

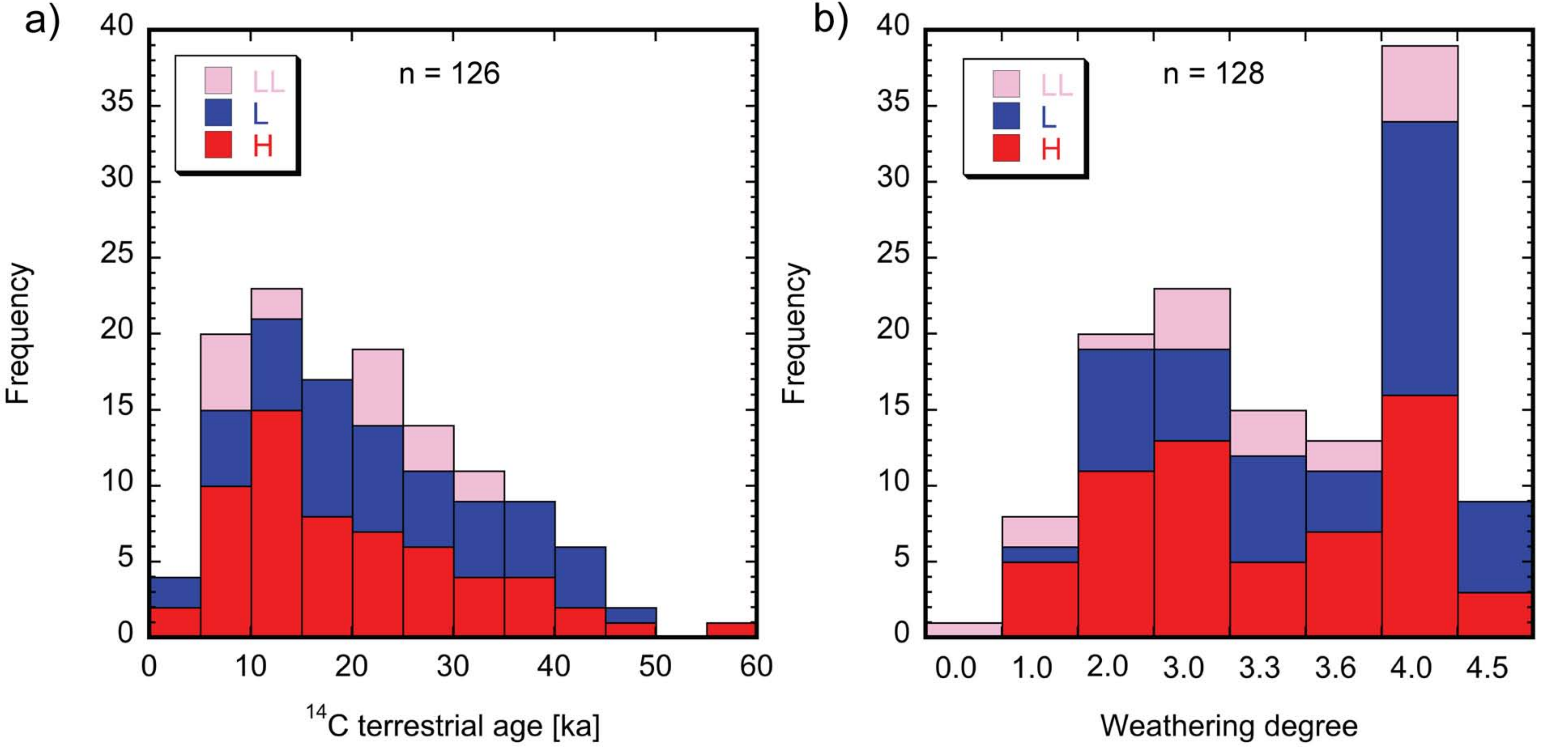
a)
b)
Frequency
n = 126
n = 128
LL
L
H
0
5
10
15
20
25
30
35
40
0
10
20
30
40
50
60
^{14}C terrestrial age [ka]
0.0
1.0
2.0
3.0
3.3
3.6
4.0
4.5
Weathering degree

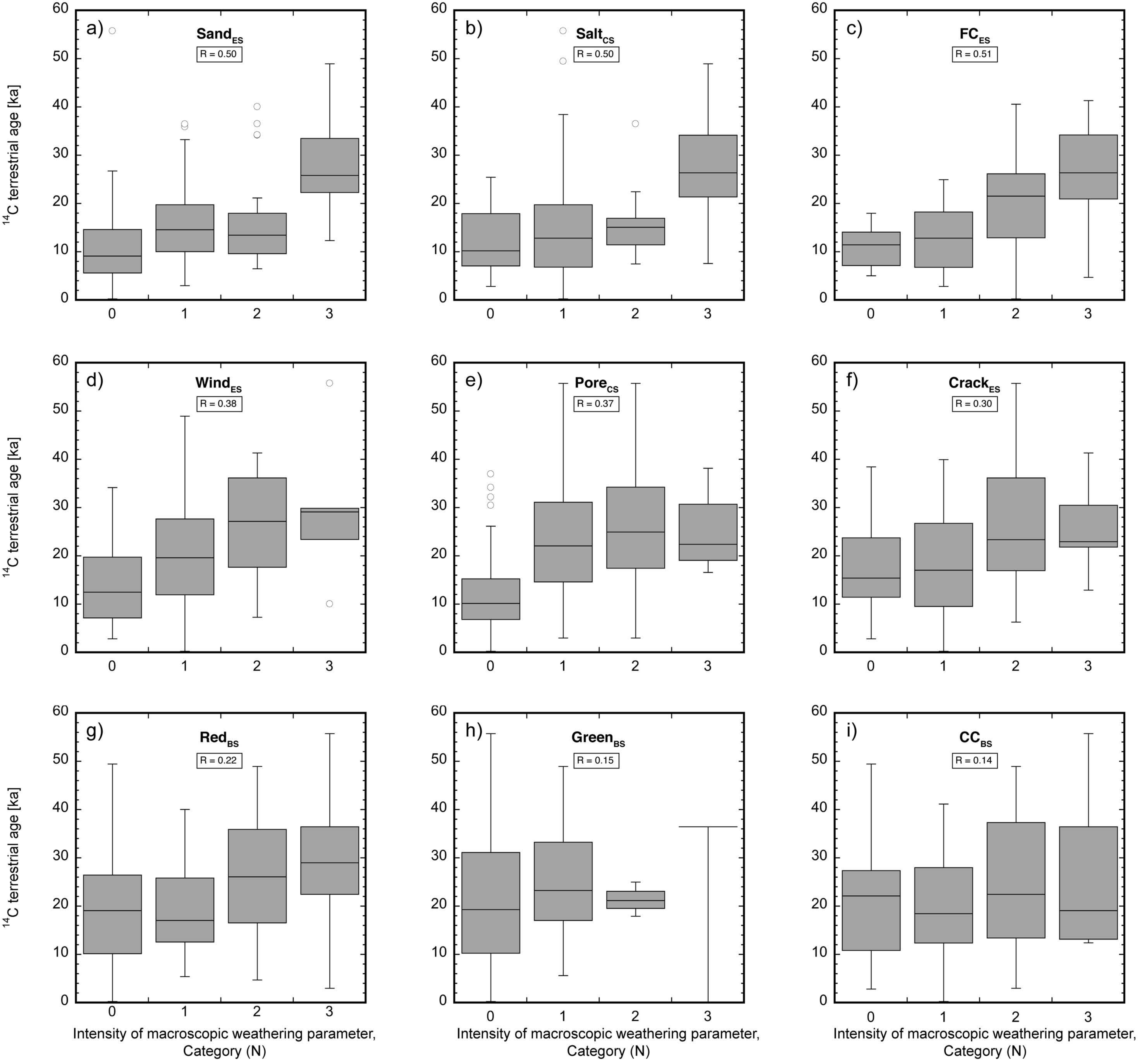

a) $Sand_{ES}$ R = 0.50
b) $Salt_{CS}$ R = 0.50
c) FC_{ES} R = 0.51
d) $Wind_{ES}$ R = 0.38
e) $Pore_{CS}$ R = 0.37
f) $Crack_{ES}$ R = 0.30
g) Red_{BS} R = 0.22
h) $Green_{BS}$ R = 0.15
i) CC_{BS} R = 0.14
^{14}C terrestrial age [ka]
0
10
20
30
40
50
60
0
1
2
3
Intensity of macroscopic weathering parameter, Category (N)

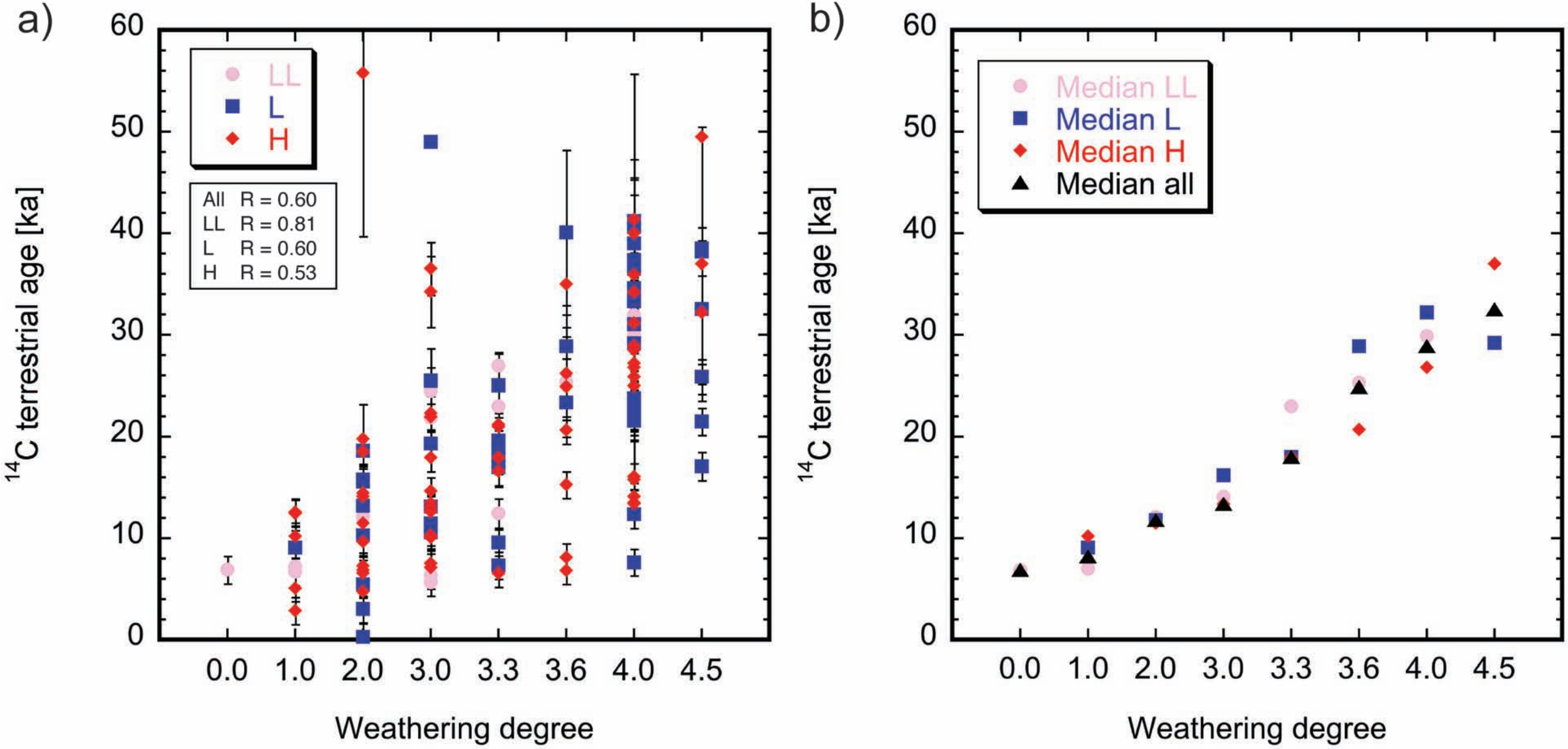
a)
LL
L
H
All R = 0.60
LL R = 0.81
L R = 0.60
H R = 0.53
^{14}C terrestrial age [ka]
0
10
20
30
40
50
60
0.0
1.0
2.0
3.0
3.3
3.6
4.0
4.5
Weathering degree
b)
Median LL
Median L
Median H
Median all
^{14}C terrestrial age [ka]
0
10
20
30
40
50
60
0.0
1.0
2.0
3.0
3.3
3.6
4.0
4.5
Weathering degree

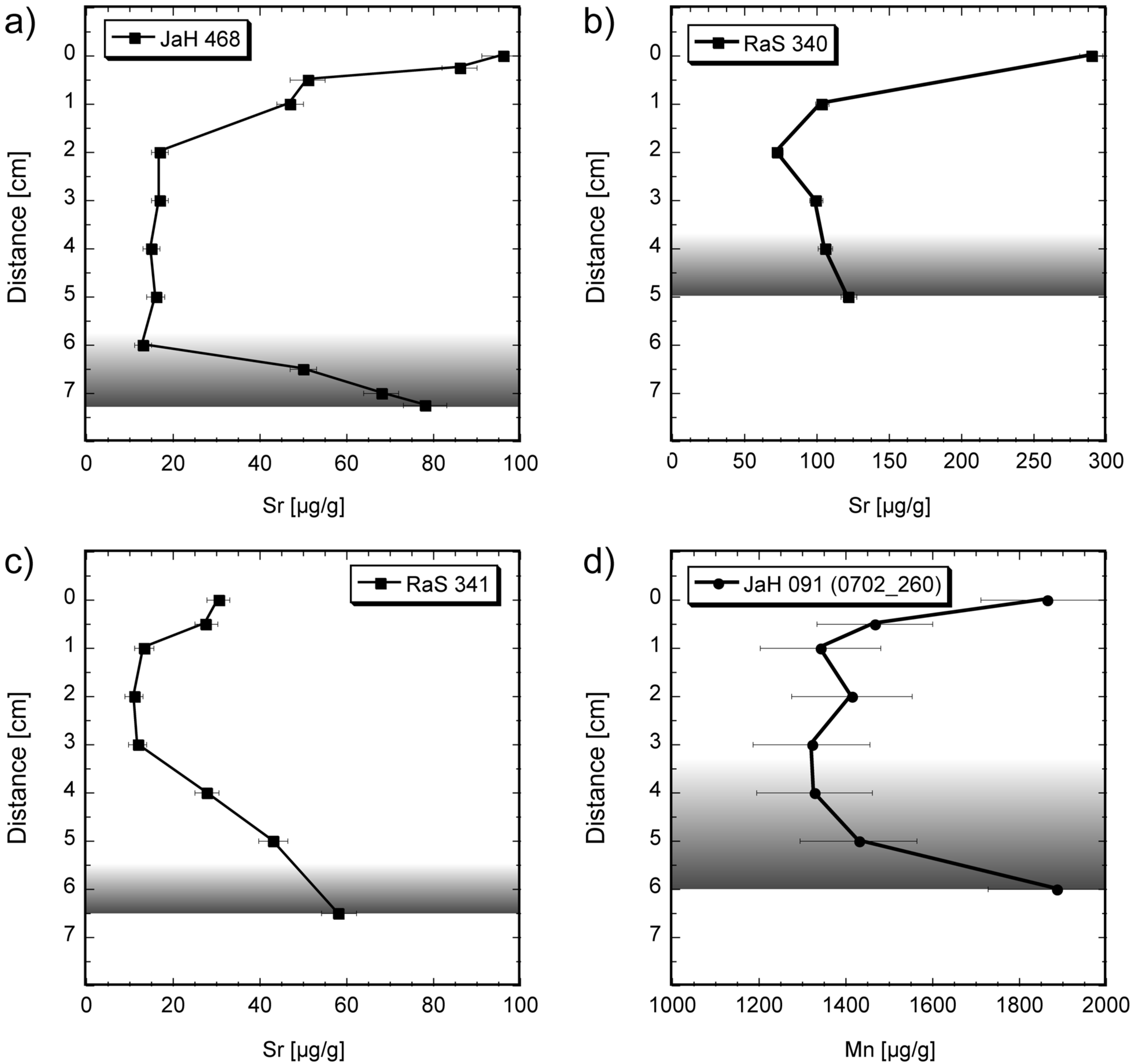

a)
JaH 468
Distance [cm]
Sr [µg/g]
b)
RaS 340
Distance [cm]
Sr [µg/g]
c)
RaS 341
Distance [cm]
Sr [µg/g]
d)
JaH 091 (0702_260)
Distance [cm]
Mn [µg/g]

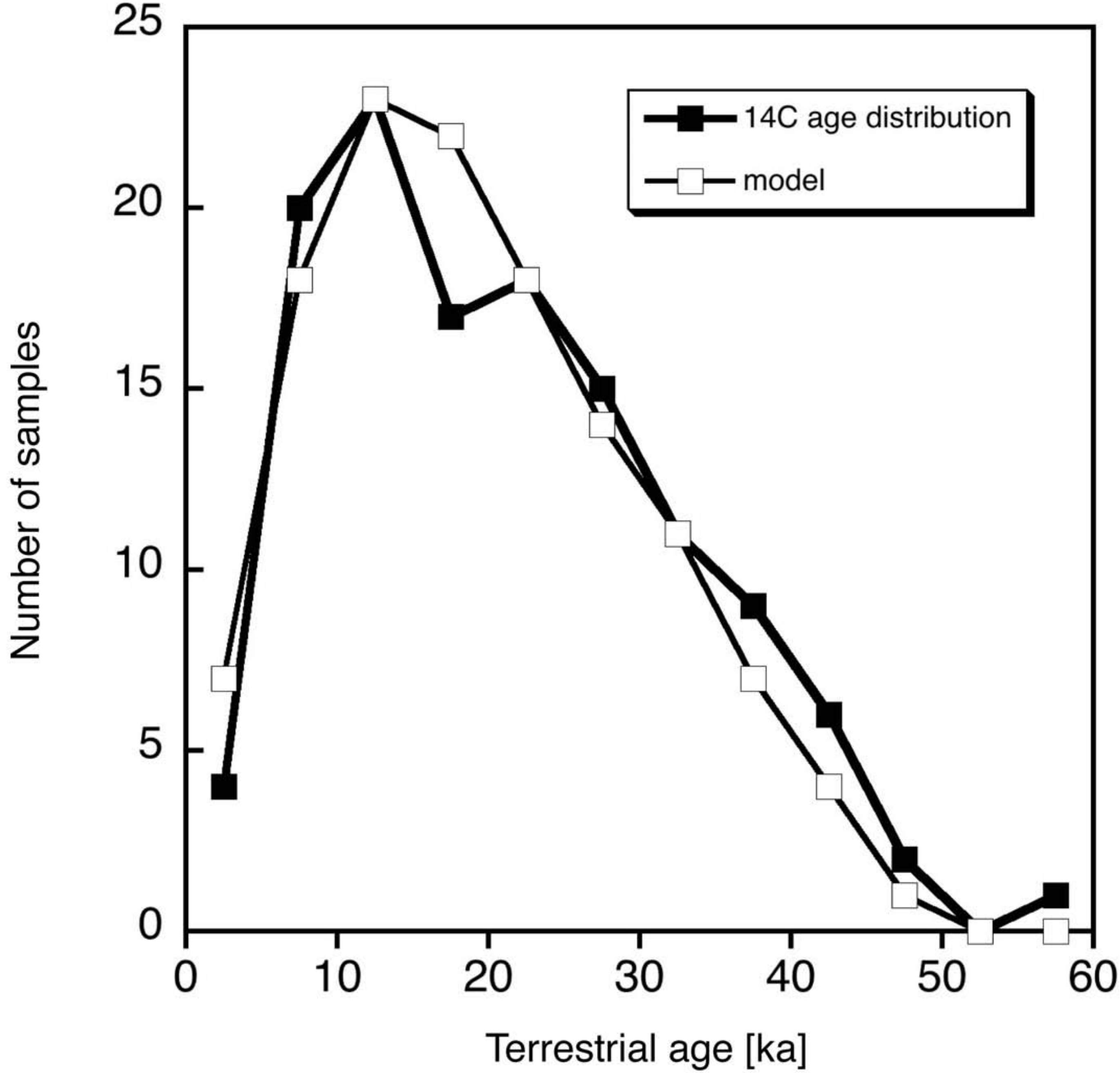

25
20
15
10
5
0
0
10
20
30
40
50
60
14C age distribution
model
Number of samples
Terrestrial age [ka]

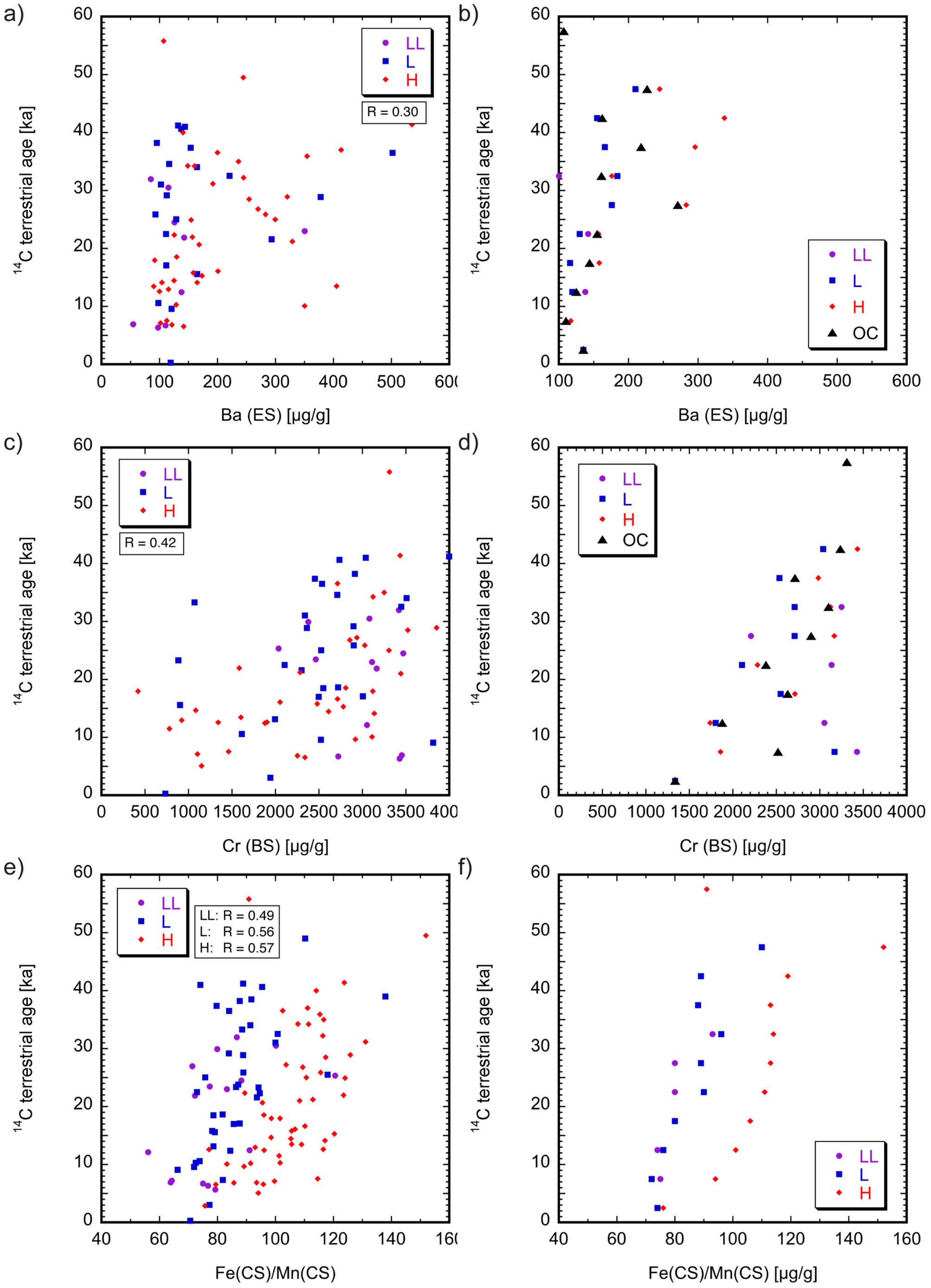

a)
LL
L
H
R = 0.30
^{14}C terrestrial age [ka]
Ba (ES) [µg/g]
b)
LL
L
H
OC
^{14}C terrestrial age [ka]
Ba (ES) [µg/g]
c)
LL
L
H
R = 0.42
^{14}C terrestrial age [ka]
Cr (BS) [µg/g]
d)
LL
L
H
OC
^{14}C terrestrial age [ka]
Cr (BS) [µg/g]
e)
LL
L
H
LL: R = 0.49
L: R = 0.56
H: R = 0.57
^{14}C terrestrial age [ka]
Fe(CS)/Mn(CS)
f)
LL
L
H
^{14}C terrestrial age [ka]
Fe(CS)/Mn(CS) [µg/g]

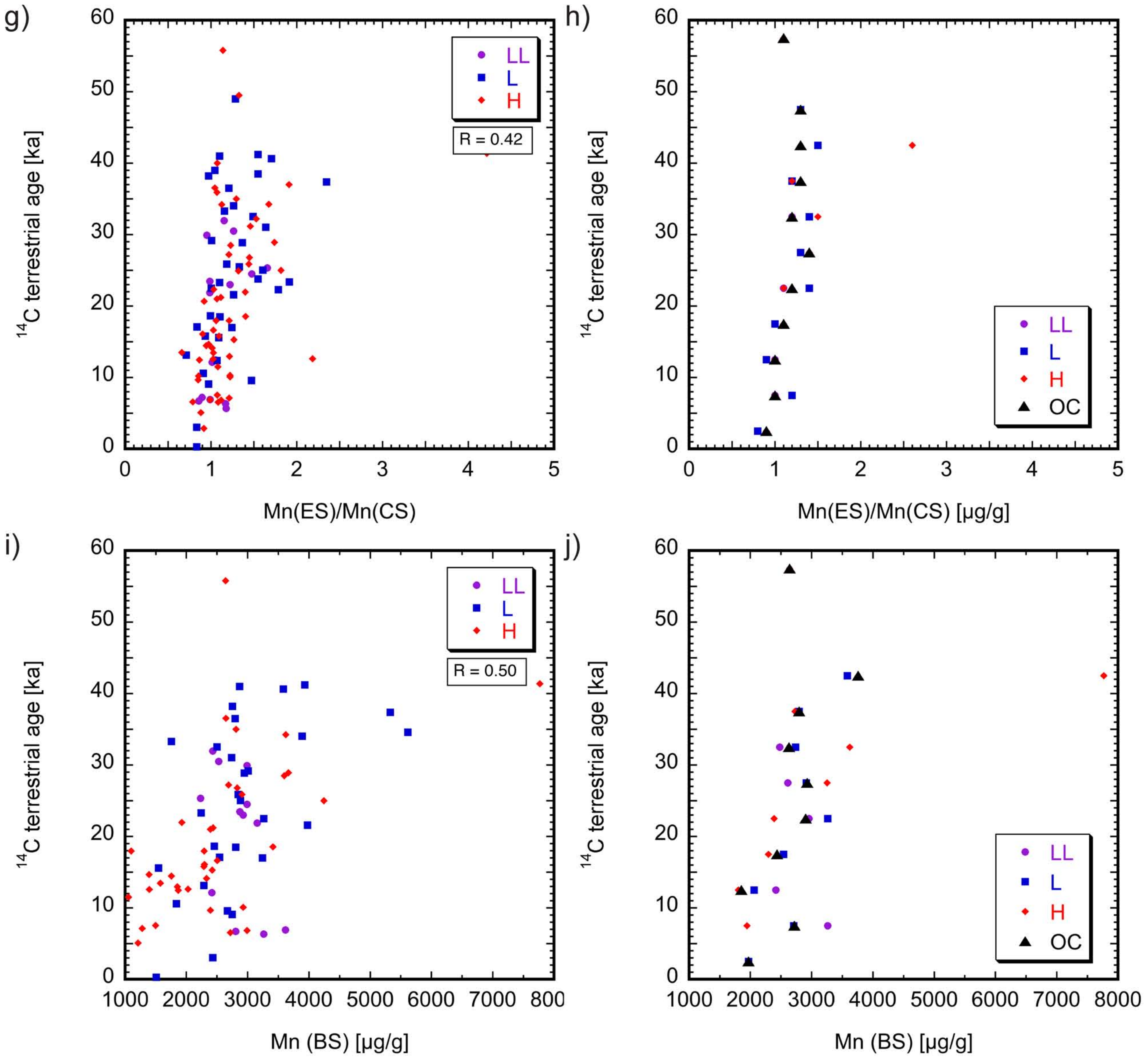
g)
LL
L
H
R = 0.42
^{14}C terrestrial age [ka]
Mn(ES)/Mn(CS)
h)
LL
L
H
OC
^{14}C terrestrial age [ka]
Mn(ES)/Mn(CS) [µg/g]
i)
LL
L
H
R = 0.50
^{14}C terrestrial age [ka]
Mn (BS) [µg/g]
j)
LL
L
H
OC
^{14}C terrestrial age [ka]
Mn (BS) [µg/g]

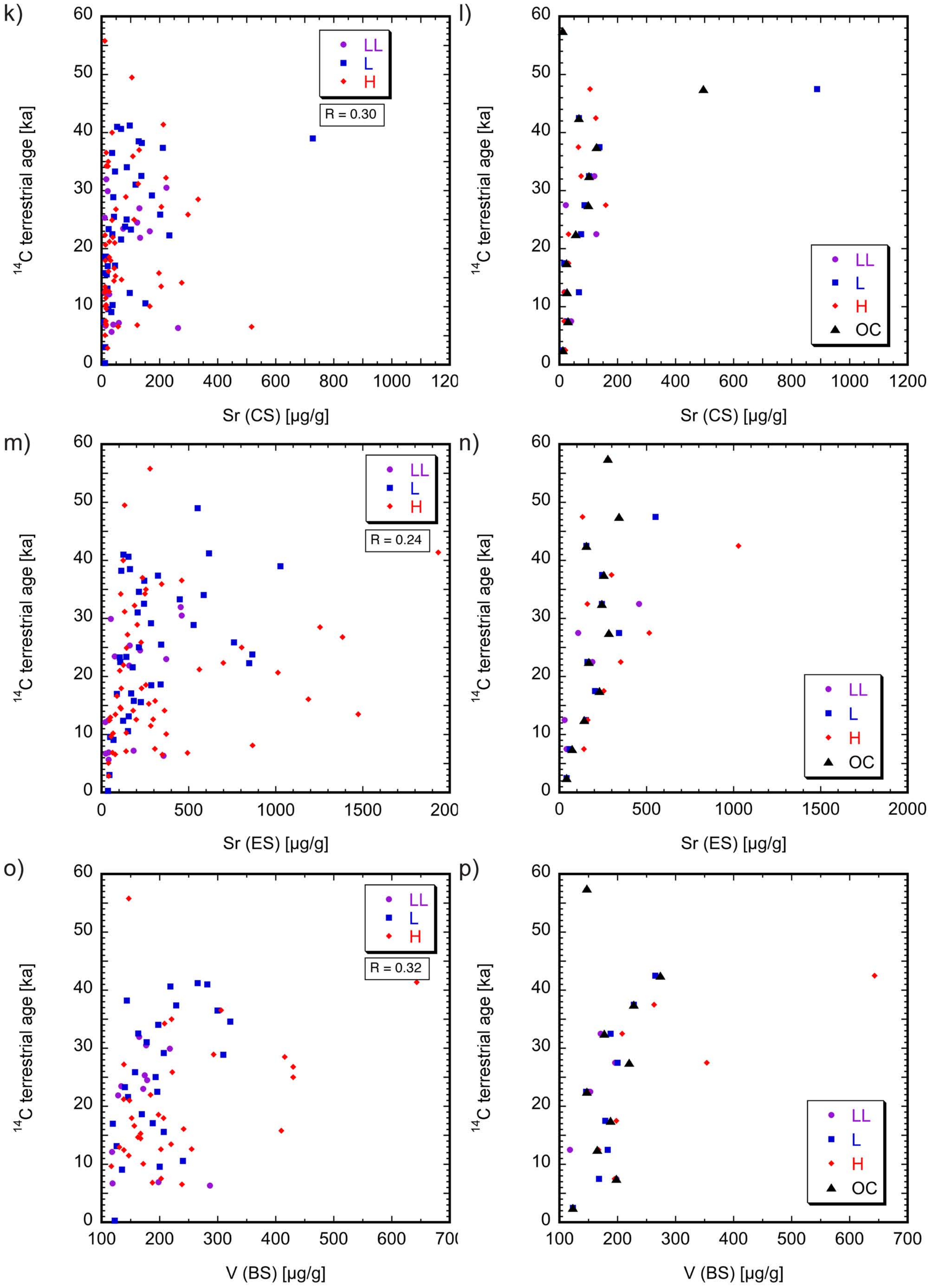

k)
LL
L
H
R = 0.30
^{14}C terrestrial age [ka]
Sr (CS) [µg/g]
l)
LL
L
H
OC
^{14}C terrestrial age [ka]
Sr (CS) [µg/g]
m)
LL
L
H
R = 0.24
^{14}C terrestrial age [ka]
Sr (ES) [µg/g]
n)
LL
L
H
OC
^{14}C terrestrial age [ka]
Sr (ES) [µg/g]
o)
LL
L
H
R = 0.32
^{14}C terrestrial age [ka]
V (BS) [µg/g]
p)
LL
L
H
OC
^{14}C terrestrial age [ka]
V (BS) [µg/g]

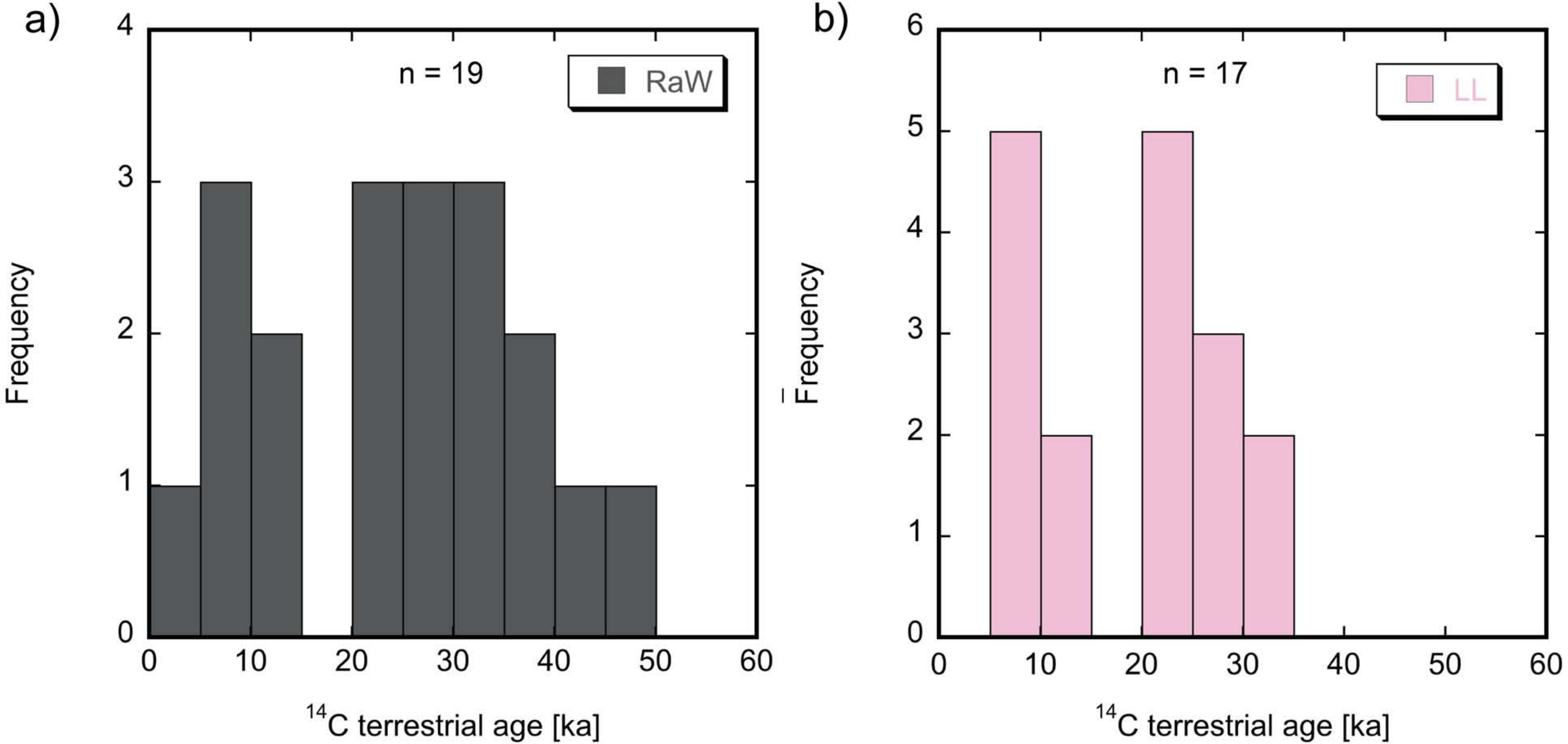
a)
n = 19
RaW
Frequency
0
1
2
3
4
0
10
20
30
40
50
60
^{14}C terrestrial age [ka]
b)
n = 17
LL
Frequency
0
1
2
3
4
5
6
0
10
20
30
40
50
60
^{14}C terrestrial age [ka]

FieldNo_Main	Name_Main	PG	N_dec	E_dec	Mass_tot	FragBE	Class	Petro	Shock	WD	WD_nr	Burial	SrM_CS	BaM_CS	FeM_CS	NiM_CS	MnM_CS	CrM_CS	CaM_CS	KM_CS	TiM_CS	VM_CS	SrM_BS	BaM_BS
0101_002	SaU_163	2	21.03703	57.32685	1877.3	36	H	5	1/2	3.3	4		27		249208	12378	2207	3032	13828		510	133	201	128
0101_006	SaU_165	4	21.02018	57.21147	457.2	3	L	5	3	4.0	6		116		231792	7286	2318	3647	14415	1368	755	131	97	103
0101_008	JaH_069	6	19.34585	56.16567	250.9	10	H	5	1/2	4.0	6		333		268835	12796	2291	2940	14819	1101	691	126	1713	240
0101_023	Dho_787	306	19.02922	54.54473	382.5	18	H	4	1/2	4.0	6		197		263935	10893	2499	4181	19154	1494	802	140	568	261
0101_049	Dho_794	11	19.05162	54.46338	431.8	1	H	6	1	4.0	6		24		258742	10843	2424	2478	12584	932	704		919	112
0101_052	Dho_020_p	306	19.04988	54.48602	82.6	1	H	4/5	3	4.0	6		205		239236	10265	2267	3271	14682	1039	715	120		
0101_124	Dho_1005	306	19.06285	54.49708	35.4	1	H	3	4	4.0	6													
0101_133	Dho_799	14	19.07040	54.53838	56.1	1	H	4	2	3.0	3		16		259415	11709	2552	3436	11827		711	129		
0101_139	Dho_802	13	19.05233	54.54195	199.4	1	H	6	3	2.0	2		26		247948	11664	2582	3293	14263	1056	639	139	492	100
0101_148	Dho_806	23	18.56528	54.08070	117.2	1	L	5	3	4.0	6		97		232458	9864	2617	3539	15143	918	653	127	680	132
0101_151	Dho_807	18	18.50428	54.08590	1260.0	1	H	5	1	2.0	2		11		230279	11123	2535	3641	13182	883	622	177	143	
0101_153	Dho_999	19	18.26817	54.15067	20.9	1	H	5	1	4.0	6		126	93	281714	9776	2148	3128	15758	1006	655			
0101_163	Dho_813	22	18.54970	54.12023	75.9	1	L	4-5	2	3.0	3		888	118	258476	10610	2345	2388	24407	1344	672	134		
0102_165	Shisr_015	23	18.54908	53.92290	3409.3	20	L	5	2	4.0	6		36		213510	8258	2542	3304	15946	1127	733	104	213	502
0102_179	Dho_005_p	20	18.17078	54.16207	122.6	4	L	6	4	4.0	6												186	117
0102_200	Dho_005_p	20	18.16850	54.15862	407.1	1	L	6	4	4.0	6		67		229651	5330	2405	2334	14998	895	630		85	138
0102_205	Dho_005_p	20	18.17358	54.15885	277.1	9	L	6	4	4.0	6		211		211790	5421	2656	3156	18781	1347	770	132	163	154
0102_207	UaH_002	25	18.50000	52.16667	96.2	1	H	3	1/2	1.0	1		12		243789	9592	2667	3965	14998	1020	703	140		
0102_218 (216)	SaU_001_p	26	20.52847	56.67448	28.1	1	L	4-5	3	2.0	2													
0102_227	SaU_194	28	21.03578	57.32825	198.4	1	L	6	2/3	4.0	6		87		223647	5138	2449	3026	18037	998	723	126	117	165
0102_231	Dho_814	32	18.96220	54.59012	99.8	1	H	5	2	2.0	2												57	
0102_234	Dho_816	32	18.97923	54.62818	23.9	1	H	5	2	2.0	2		57		254391	11379	2655	3554	17023		785	134		
0102_253	Shisr_017	35	18.42322	53.60905	12.8	1	H	4	5	4.0	6		108		250111	11120	2169	3728	18961		598	135		
0102_256	Shisr_020	38	18.55927	53.89155	2200.7	4	H	4-6	3	3.0	3		16		246059	12373	2400	3492	12365		714		1546	221
0102_258	Dho_835	10	18.64482	54.00393	160.1	1	H	5	1/2	4.0	6		50		257106	13380	2349	3024	14308		583	120	671	172
0103_259	Shalim_004	40	18.18233	55.50183	10350.0	50	H	5	1/2	3.0	3		14		235979	10667	2536	2983	15476	772	766	107	48	
0201_0077	Shisr_025	44	18.10740	53.83190	7293.5	1	L	6	3	2.0	2													
0201_0083	Shisr_028	46	18.14277	53.80753	818.1	11	LL	6	3	4.0	6													
0201_0108	JaH_102	55	19.51185	56.98178	1007.3	67	H	5	2	4.0	6		213	96	265080	9562	2142	3911	16663	1127	692	148	1481	260
0201_0135	SaU_189	64	20.60242	57.37903	694.9	1	LL	7	5	4.0	6		74		211165	10293	2731	3230	16261	967	589	130	113	
0201_0508	JaH_120_p	310	19.73335	55.72442	1070.7	1	H	5	1	2.0	2		14		262454	11792	2593	3148	12829	886	697	117	407	
0201_0592	JaH_073_p	70	19.73560	55.71775	7920.0	1	L	6	4	3.3	4													
0201_0640	JaH_073_p	70	19.70928	55.73078	1200.0	1	L	6	4	3.3	4													
0201_0642	JaH_073_p	70	19.71150	55.73053		1	L	6	4	3.6	5													
0201_0664	JaH_073_p	70	19.70742	55.73615	1053.9	1	L	6	4	3.0	3													
0201_0788	AH_011	71	19.86607	57.00320	8175.0	1	L	6	4	2.0	2		12		210467	9290	2725	2924	13863	1104	578	102	13	
0201_0821	JaH_073_p	70	19.63793	55.74793		0	L	6	4	4.5	7													
0201_1217	Aybut_001	72	17.75793	53.99032	442.3	1	H	6	2	1.0	1		12		238402	10221	2534	3322	14092	975	655	112	130	
0209_0004	SaU_219	111	20.48407	56.94290	2934.0	1	H	4	1	3.6	5		48		262923	11977	2185	3394	15341	847	629		146	
0209_0013	SaU_228	121	20.50222	57.37372	450.9	1	H	6	1	2.0	2		16		240583	9130	2698	3281	14890	1162	767	118	44	87
0210_0011	JaH_091	86	19.69362	56.65432	123374.4	1000	L	5	2	3.0	3													
0211_0001	SaU_264	96	20.69617	57.19490	3548.1	6	LL	6	1-2	4.0	6		22		217857	11006	2727	3049	13457		580		50	
0212_0011M	SaU_209	121	20.33168	57.24740	5590.0	1	H	5	1	2.0	2													
0212_1911	SaU_235	128	20.54182	57.19892	2370.1	80	L	6	4	4.0	6		37		204379	8547	2804	2620	16656	1335	805	109	84	111
0212_1913	SaU_259	130	20.62270	56.94792	1415.1	1	H	4	1	4.0	6		206		245974	7986	2371	3373	15247	1317	894	119	55	
0212_1946	Dho_1012	135	18.55492	54.02930	144.9	1	L	6	3	1.0	1		34		194648	4804	2936	3421	15918	1012	749	106	63	
0212_1951	Dho_1010	38	18.55417	54.00253	2298.4	1	H	4	1	3.0	3		69		243973	12377	2477	3547	17503	898	623	141	132	
0212_1970	JaH_396	144	19.99542	56.39193	122.6	2	LL	5	3	3.3	4		166		215127	7675	2584	3768	14965	1165	785	125	116	
0301_0002	Shisr_031	307	18.21335	53.84675	503.8	2	L	6	3	4.0	6		67		229352	7923	2451	3039	19008	1118	700	138	146	294
0301_0003	UaH_001	153	18.44432	52.97805	2335.6	7	LL	5	2	2.0	2		26		175189	3513	3123	2629	17677	1162	792	122	26	
0301_0005	Shisr_035	132	18.42957	54.04127	355.1	1	L	6	5	4.0	6		233		214262	4672	2264	2489	23441	1365	733	109		
0301_0018	SaU_250	113	20.58298	57.31650	16200.0	2	H	4-6	2	3.3	4		45		253307	12697	2338	2809	13831		639	121	77	
0301_0037	RaS_204	173	20.62820	56.19198	9050.0		L	6	4	4.0	6		101		226904	6706	2409	2718	15419	1468	643	111	61	
0301_0038	RaS_205	174	20.62973	56.16912	742.8	2	L	6	5	2.0	2		13		218162	9627	2790	3180	13029	996	694	155		
0301_0044	RaS_211	178	20.58587	55.87252	143.0	1	LL	6/7	1	3.0	3		133		195832	5945	2711	3021	23364	1057	804	137	118	96
0301_0049	RaS_216	173	20.57445	55.98598	584.9	4	L	6	4	4.5	7		138		224700	6044	2563	3303	16177	1139	739	118	97	96
0301_0050	JaH_078	182	19.91448	55.66278	882.7	1	L	6	4	2.0	2		15		215218	9013	2633	2884	14402	942	714	122	435	
0301_0061	RaS_113	189	20.46543	55.86245	1499.0	1	L	6	2	3.0	3		21		215315	8755	2741	3080	17813	1105	825	117	113	
0301_0066	RaS_114	177	20.56848	56.10217	142.4	1	H	5	1-2	3.6	5		14		251061	14035	2628	2899	11691		654	117		
0301_0068	RaS_226	193	20.56250	56.08372	632.4	1	L	6	2	4.0	6		173		221456	8597	2639	3173	19398	1056	772		326	113
0301_0074	RaS_232	197	20.55215	55.92297	350.3	5	H	5	3	4.0	6		276		261983	13049	2237	3019	15417	1012	598	132		
0308_0001	Shisr_032	200	18.04100	53.69267	69.5	1	H	5	2	1.0	1		10		251435	11983	2616	3280	12651	1142	646		50	
0502_031	RaS_242	216	20.01798	56.41798	96.6	1	LL	4	3	3.0	3	60	122		232292	12050	2633	3957	15741	1093	648	128	1636	119
0502_043	QaM_001	223	21.37015	57.72910	7269.0	1	LL	4-6	2	3.0	3	70	264		212550	8515	2768	3330	19586	1042	707	123	1128	131
0503_116	SaU_420	255	20.92243	56.88684	188.8	2	LL	6	2	3.3	4		11		243849	12227	2677	2645	11557	1003	520	145		
0603_021	RaW_002	273	21.37030	58.40459	475.2	5	H	4/5	2	2.0	2	80	43	107	246015	12200	2335	3731	21301		735	129	104	112
0603_025	RaW_005	274	21.22514	58.41161	56.6	1	H	5	3	4.0	6	20	22		243442	16066	2184	3852	13797		743			
0603_027	RaW_007	275	21.17461	58.40919	1940.7	111	H	5	2	4.0	6		298		262241	8397	2270	4017	15203	1082	716	120	134	279
0603_028	RaW_008	276	21.16830	58.39144	7.8	1	L	4	2	3.0	3		43	112	262093	11999	2222	3330	13965	904	696	131		
0603_031	RaW_010	277	21.13830	58.36359	23.2	2	H	4	2/3	4.0	6		112		259838	10678	2347	3297	15545		640	133	927	210
0603_035	RaW_014	278	21.05979	58.40432	5591.0	1	H	5	2	2.0	2	20	16		237753	12253	2542	3358	14518	930	761	145		
0603_037	RaW_015	273	21.17277	58.42175	295.8	1	H	5	3	3.0	3	0	12		263112	13204	2414	3130	11750		637		135	125
0603_038	RaW_016	279	21.16639	58.41034	115.4	12	L	6	4/5	4.5	7	80	136		224982	4934	2233	2931	15119	1098	757		151	221
0603_039	RaW_017	280	21.15840	58.38922	70.1	1	H	5	2	3.0	3	0	14		248035	11977	2487	3740	13502	827	646	150	54	
0603_041	RaW_019	281	21.21272	58.38638	546.1	49	H	6	1	4.5	7	50	222		266449	9359	2291	2617	15148	1338	604	160		
0603_043	RaW_021	282	21.15200	58.41393	59.1	1	H	5	1	4.0	6	0	84	106	271067	7798	2154	3059	12915	859	738		221	313
0603_044	RaW_022	283	21.49311	58.46440	89.9	1	H	5	3	4.0	6	10	36		260393	9216	2282	3270	15573	912	771	114		
0603_046	RaW_024	284	21.37628	58.42769	12.1	1	H	5	2	1.0	1	10	20		227059	8711	2999	4033	16066	922	764	129		
0603_050	RaW_027	286	21.26005	58.39152	1174.4	102	H	5	2/3	4.5	7	30	129		247302	7546	2226	3122	15273	888	681	179		
0603_053	RaW_031	287	21.27326	58.39645	195.3	1	H	4	2	3.0	3	0	38		267975	11002	2170	3775	14231		662		99	202
0603_054	RaW_032	288	21.33802	58.41154	13.5	1	L	6	4	4.5	7		128	186	232677	6500	2538	4436	25443	975	770	129		
0603_056	RaW_034	289	21.36230	58.41178	61.1	1	LL	3-5	2	0.0	0	5	40		192759	3760	3018	4302	18561	1357	809	124	65	91
0603_057	RaW_035	290	21.36865	58.39767	30.7	1	H	5	2	3.6	5		36		265452	12658	2140	3661	14242	1129	594	128		
0603_060	RaW_038	285	21.37054	58.41401	7.4	1	H	5	2	4.5	7	0	105	147	305938	10118	2013	3524	16735		568	123		
0603_179	RaS_262	299	20.01351	56.40696	425.0	1	LL	6	3	1.0	1	30	59		192284	4930	2991	3246	17975	1100	733	113		
0603_221	JaH_343	300	19.75174	56.57984	528.4	3	LL	6	3	1.0	1		13		213269	8522	2844	4025	15325	1010	748	120	56	
0603_250	Al_Huqf_063	304	19.44534	57.02345	591.8	1	L	6	2	3.6	5	0	24		223490	9314	2586	3130	14637	851	649	109		
0702_007	JaH_413	418	19.82991	56.57698	172.6	1	H	4	1	3.0	3		26		269362	11931	2312	3173	12799	935	671		734	151
0703_016	JaH_493	314	19.78449	56.41668	438.7	4	L	6	3/4	3.3	4		86		209811	7915	2770	3083	18049	1024	769		186	129
0703_017	JaH_416	427	19.78721	56.42156	18.8	1	L	6	5	4.0	6		81		223878	6546	2568	3722	14662	1035	783	129		
0703_019	JaH_418	313	19.79234	56.42625	205.9	1	H	4	3	3.6	5	50												
0703_029	JaH_423	319	19.78329	56.41394	1457.3	1	H	4	3	3.3	4	15	31		242136	11518	2384	3522	14121		650	151	366	289
0703_031	JaH_498	314	19.79219	56.40977	59.5	1	L	6	4	3.6	5	50	40		226462	8350	2548	3335	15667	994	768		492	378
0703_035	Al_Huqf_065	320	19.32091	57.22976	2084.2	41	L	6	5	2.0	2		12		202150	8395	2865	2981	14173	1119	737	123	48	119
0703_541	JaH_474	358	19.81418	56.44561	226.8	1	LL	3.7-6	2	3.0	3	15	34		212340	4957	2678	3620	16224	2585	731			
0801_005	RaS_267	368	20.59710	56.15087	117.1	6	LL	6	1	4.0	6	10	223		221949	4831	2216	3132	19901	1276	688	108	889	103
0901_003	RaS_281	429	20.57092	56.38846	203.7	1	H	3-6	3	3.0	3	35	13		231308	11313	2345	3677	13276		709		137	
0901_007	UaS_009	432	21.06494	56.48188	3989.0	1	L	6	4	4.0	6	85	46		223882	5794	2530	3856	15236	1286	801		58	
0901_010	UaS_011	435	21.37603	56.29112	790.5	1	H	4	1	3.0	3	0	12		239781	11222	2681	3461	13468	893	666	114		
0901_012	UaS_013	436	21.37280	56.31376	205.6	1	L	6	4	2.0	2	0	17		214745	9620	2716	3195	15412	1044	751	133	2026	165
0901_026	RaS_290	449	20.52340	55.53072	446.8	2	L	6	4	3.3	4	60	12		216032	9609	2748	3215	14825	1160	656	109	144	
0901_028	RaS_292	451	20.59832	55.52398	1991.7	5	L	6	2	3.0	3	50	151		211524	8364	2865	3456	14439		770		204	98
0901_031	RaS_295	454	20.66974	55.42814	227.7	1	H	4	2	3.0	3	30	15		269267	12859	2350	3626	14295		636	160	1160	95
0901_033	RaS_297	455	20.66748	55.31715	706.9	20	L	6	4	4.5	7	40	202		217141	5632	2441	2830	17923	1177	616		302	93
0901_038	RaS_302	457	20.14475	56.24085	161.7	1	H	4	2	3.6	5	0	23		247346	11497	2121	3604	13540		609	133	271	119
0901_040	RaS_304	459	20.43802	56.10279	373.4	2	H	6	2	3.3	4	30	43		253343	9985	2299	2839	13051	1436	686		108	98
0901_055	JaH_578	466	19.76420	56.29889	1064.3	1	H	6	2	1.0	1	85	14		219927	7542	2852	3414	15301	1074	806	140	193	
0901_059	Al_Huqf_069	469	19.26795	57.13411	250.5	1	H	4/5	2	3.0	3	80	16		249787	12323	2318	3378	13094	882	637	131	324	121
0901_060	JaH_579	470	19.35421	56.75286	475.1	27	L	4-6	3-5	3.3	4	30	24		206141	8686	2868	3836	16789	1086	721	120	112	121
0902_081	JaH_595	477	19.50875	56.64635	929.1	1	L	5	3	3.6	5	5												
0902_098	Shalim_008	488	18.86795	55.45073	323.5	1	H	5	3	2.0	2	50												
0902_113	JaH_620	499	19.37127	56.36915	244.6	3	L	6	4	2.0	2	5	38	554	281091	9213	3877	1659	11150	378	572	131		
0902_119	RaS_310	504	20.78308	55.44327	1223.2	6	H	3.2-6	3	2.0	2													
0902_125	RaS_316	506	20.89485	55.50613	2706.0		L	5	3	4.5	7		46		217759	6684	2482	3534	17054	1107	683	96	228	112
0902_131	RaS_322	510	20.91903	55.41193	264.4	1	H	3.7	1	3.0	3	40	166		215127	7675	2584	3768	14965	1165	785	125	116	
0902_139	SaU_519	516	20.37165	56.51017	403.2	18	L	5	3	4.0	6	25	54		205456	8540	2774	3762	16974	1483	673	133	293	144
0902_146	SaU_523	348	20.41533	56.66550	265.2	1	L	6	4	3.3	4	20	21		220928	8984	2581	2851	14241	965	665	104	114	
0912_001	Al Huwaysah 001	522	22.80487	55.32742	3150.5	237	LL	6	3	4.0	6	50	16		224574	11290	2591	3639	13565		643	128	609	
1001_080	RaS_370	443	20.50627	55.82513	182.4	1	LL	6	2	3.6	5	60	185		256580	11039	2393	3246	14269	1350	687	136		
1001_099	JaH_643	590	19.60592	56.69978	132.8	1	LL	6	2	3.3	4	20	130	98	285751	10199	4006	4317	62951	1827	1143	189		
1001_102	RaS_385	592	20.05473	56.46193	2275.3	5	LL	3.3	1	3.6	5	10	11		263164	11759	2183	2631	11912		570		190	
1002_121I	RaS_393	610	20.14600	55.70941	2.2	1	H	6	2	3.6	5													
1002_121N	RaS_394	609	20.14724	55.70960	0.2	1	H	4	3	3.6	5		122	99	215213	7712	2512	2477	16511	1046	736	126	364	127
1002_123	RaS_395	608	20.14690	55.70922	982.5	3	L	6	5	4.0	6	80												
1002_124	RaS_396	611	20.14690	55.70908	30.3	1	H	4	2	3.3	4	60	517		211448	7611	2661	2928	16669	1098	741	120	282	123
1002_125	RaS_397	608	20.14650	55.70913	1118.8	273	L	6	5	4.0	6		97		214049	9246	2535	2816	28822	3867	1115	117		
1002_126	RaS_398	608	20.14673	55.70975	289.6	23	L	6	5	4.0	6	50	728		297038	13595	2154	2437	13019		594	190		
1002_127	RaS_399	612	20.15122	55.70925	6319.0	1	L	6	2	3.3	4	0	9		222186	10966	2714	3613	13805	894	758			

FieldNo_Main	Mn(ES)/Mn(CS)	Fe(CS)/Mn(CS)	V(ES)/V(CS)	Sr(ES)/Sr(CS)	Sr(ES)/Ba(ES)	Fe(ES)/Mn(ES)	Fe(CS)/Ni(CS)	Fe(ES)/Ni(ES)	Ni(ES)/Ni(CS)	Ca(ES/Ca(BS)	Salt_CS_rev	Porefill_CS	Red_dorso_BS	Ni_green_stain_BS	FC_BS_alt	FC_ES_alt	FC_ES_neu
0101_002	1.1	112.9	2.6	20.8	1.7	106.5	20.1	20.1	1.3	0.5	3	2	2	2	1	1	2
0101_006	1.6	100.0	2.6	1.8	1.7	58.8	31.8	31.8	1.8	1.1	3		2	1		0	3
0101_008	1.2	117.3	2.9	3.8	4.9	90.4	21.0	21.0	1.0	0.7	3		1	0		0	3
0101_023	1.1	105.6	2.2	1.6	1.9	95.5	24.2	24.2	1.2	0.9	3	1	1	0		1	2
0101_049	0.9	106.7		49.7	5.9	123.6	23.9	23.9	1.2	1.4	1	1	0	0	0	0	3
0101_052	0.7	105.5	3.8	7.2	3.6	210.4	23.3	23.3	1.4		3	2	2	1	0	1	2
0101_124											3	2	0	0	1	0	3
0101_133	1.2	101.6	1.7	8.7	1.1	81.3	22.2	22.2	0.8		3	1	0	0	2	2	1
0101_139	1.4	96.0	1.5	9.7	2.0	64.0	21.3	21.3	1.1	0.9	1	2	1	0	2	3	0
0101_148	1.5	88.8	2.6	6.4	4.8	50.8	23.6	23.6	0.8	1.2	3	2	2	1	0	0	3
0101_151	1.1	90.8	1.0	24.5	2.6	79.6	20.7	20.7	0.9	1.2	1	2	3	0	1	0	3
0101_153	1.5	131.1		1.0	0.7	92.0	28.8	28.8	1.4		3	2	0	0			
0101_163	1.3	110.2	1.5	0.6	2.6	67.4	24.4	24.4	0.7		3	2	2	1			
0102_165	1.2	84.0	2.2	6.9	2.1	64.2	25.9	25.9	1.3	3.6	3	2	3	3	3	1	2
0102_179					1.5	33.4				1.2	3	2	2	0	0	1	2
0102_200	1.7	95.5		2.3	0.8	55.7	43.1	43.1	1.8	1.8	3	2	2	0	1	1	2
0102_205	2.3	79.7	2.2	1.5	1.7	36.2	39.1	39.1	1.3	1.4	3	2	2	0	2	1	2
0102_207	0.9	91.4	1.1	5.4		114.1	25.4	25.4	1.3		0	0					
0102_218 (216)											1	1	1	0	3	2	1
0102_227	1.3	91.3	1.7	6.8	3.2	71.2	43.5	43.5	1.2	1.3	3	2	2			1	2
0102_231					1.7	79.6				1.3	1	0		0			
0102_234	0.8	95.8	1.0	1.4		125.3	22.4	22.4	0.7		0	0	0		3	3	0
0102_253	1.1	115.3	2.6	3.2	1.0	111.0	22.5	22.5	1.1		3	1	0	0	0	0	3
0102_256	1.0	102.5		29.2	2.3	100.9	19.9	19.9	0.9	0.7	2	1	1	0	1	1	2
0102_258	1.4	109.4	5.4	27.9	5.1	75.7	19.2	19.2	0.8	0.5	1	2	0	0	3	3	0
0103_259	1.2	93.0	1.4	3.7	0.4	97.2	22.1	22.1	1.3	0.7	2	1	1	0	1	1	2
0201_0077											1	2	2	1	2	2	1
0201_0083											3	1	3		0	1	2
0201_0108	4.2	123.8	4.6	9.1	3.6	30.0	27.7	27.7	1.4	1.3	3	2	0	0	0	0	3
0201_0135	1.0	77.3	0.9	1.0		76.9	20.5	20.5	0.6	1.2	3	2	0	0	0	0	3
0201_0508	1.1	101.2	1.6	20.2		93.8	22.3	22.3	0.9	1.5	2	1			2	3	0
0201_0592											3	2	2	0	2	0	3
0201_0640											3	2	1	1	3	3	0
0201_0642											3						
0201_0664											1	2	2	0	0	1	2
0201_0788	0.8	77.2	1.2	3.7		99.7	22.7	22.7	1.0	1.1	1	2	3	0	3	1	2
0201_0821																	
0201_1217	0.9	94.1	1.4	3.3		123.3	23.3	23.3	1.2	0.1	1	1	3	0	3	3	0
0209_0004	1.3	120.3		5.7	1.6	92.3	22.0	22.0	1.5	1.1	1	0	1		1	1	2
0209_0013	0.8	89.2	1.1	3.4		109.6	26.4	26.4	1.3	0.9	2		0		0	1	2
0210_0011											1	2	1	0			
0211_0001	1.0	79.9		2.4		81.1	19.8	19.8	0.8	1.1	3	1	2	1	0	0	3
0212_0011M											1	1	2	0			
0212_1911	1.0	72.9	1.3	2.9		72.6	23.9	23.9	1.1	1.5	2	1	3		0	0	3
0212_1913	1.2	103.7	1.3	0.7		85.4	30.8	30.8	1.2	1.5	3	2	2		0	1	2
0212_1946	1.0	66.3	1.7	2.0		73.1	40.5	40.5	1.0	1.0	0	0	1		3	3	0
0212_1951	1.0	98.5	1.6	1.6		111.7	19.7	19.7	1.0	2.3	2	1	1		2	3	0
0212_1970	1.2	83.3	2.0	2.2	1.1	67.4	28.0	28.0	1.6	0.7	3	2	0	0	0	0	3
0301_0002	1.3	93.6	1.4	2.7	1.0	88.7	28.9	28.9	1.6	1.5	3	3	0		1	1	2
0301_0003	1.0	56.1	1.1	0.8		52.6	49.9	49.9	3.5	1.3	0	0	1	0	3	3	0
0301_0005	1.8	94.6	2.7	3.6	6.5	54.1	45.9	45.9	1.8		3	2	0	1	0	0	3
0301_0018	1.1	108.4	1.1	2.3		99.4	20.0	20.0	0.8	0.9	1	1	1	1	0	0	3
0301_0037	1.1	94.2	1.5	1.0	1.1	85.3	33.8	33.8	1.4	1.0	3	3	1	1	0	0	3
0301_0038	0.9	78.2	0.7	14.8		100.8	22.7	22.7	0.8		2	1	0		3	3	0
0301_0044	1.0	72.2	1.1	1.2	1.1	71.1	32.9	32.9	0.9	1.1	3	1	2		0	1	2
0301_0049	1.0	87.7	1.1	0.8		87.1	37.2	37.2	1.4	1.1	3	3	3	1	0	0	3
0301_0050	1.0	81.7	1.7	23.3	3.2	89.2	23.9	23.9	0.6	0.2	1	1	1	1	0	2	1
0301_0061	0.7	78.6	1.2	7.6		122.0	24.6	24.6	0.9	0.7	1		0		2	2	1
0301_0066	0.9	95.5	2.0	74.9	6.0	126.3	17.9	17.9	0.9		1	1	0		1	1	2
0301_0068	1.0	83.9		1.6	2.5	82.3	25.8	25.8	0.8	1.0	3	2	3		0	0	3
0301_0074	1.0	117.1	1.4	1.3	2.2	111.7	20.1	20.1	0.8		3	1	0		0	0	3
0308_0001	0.9	96.1		4.7		114.8	21.0	21.0	0.7	0.4	1	1	1	1	2	3	0
0502_031	1.5	88.2	1.7	1.8	1.8	56.9	19.3	19.3	1.0	0.3	0	1	0		1	1	2
0502_043	1.2	76.8	2.5	1.4	3.7	63.4	25.0	25.0	1.3	1.0	1	0	0		1	1	2
0503_116	1.1	91.1	1.1	3.6	0.3	86.0	19.9	19.9	1.3		1	1	1	1	0	1	2
0603_021	0.9	105.4	1.4	2.6	0.9	114.8	20.2	20.2	0.9	1.3		1	0		0	0	3
0603_025	1.1	111.5		5.1	0.7	119.9	15.2	15.2	0.8		3	0	0		1	1	2
0603_027	1.4	115.5	1.8	0.8	0.8	77.8	31.2	31.2	1.6	1.2	3	1	1		0	0	3
0603_028	1.3	118.0	3.8	8.0	0.8	97.0	21.8	21.8	0.9		0	1	0	1	0	1	2
0603_031	1.8	110.7	4.3	7.2	2.7	63.1	24.3	24.3	1.0	0.6	3	2	0		2	2	1
0603_035	1.0	93.5	1.1	4.0		93.6	19.4	19.4	0.8		1	0	0			2	1
0603_037	1.0	109.0		7.0	0.9	100.8	19.9	19.9	0.9	1.8	3	2	1		1	0	3
0603_038	1.5	100.8		1.8	0.4	75.0	45.6	45.6	1.7	0.9	3	1	0		0	0	3
0603_039	1.2	99.7	1.1	10.2	1.4	76.3	20.7	20.7	0.7	1.8	0	1	0		0	1	2
0603_041	1.5	116.3	1.3	0.9	0.8	73.6	28.5	28.5	0.9		3	0	0		0	0	3
0603_043	1.7	125.8		2.4	0.6	75.1	34.8	34.8	2.3	1.7	3	2	1		0	0	3
0603_044	1.1	114.1	1.3	3.4	0.9	114.8	28.3	28.3	1.5		3	1	0	1	0	0	3
0603_046	0.9	75.7	1.2	2.1		81.7	26.1	26.1	1.0		0	0	0		2	2	1
0603_050	1.9	111.1	1.7	1.8	0.6	63.4	32.8	32.8	1.4		3	0	1	0	0	0	3
0603_053	1.4	123.5		3.3	0.8	83.6	24.4	24.4	1.0	1.6	3	1	0	0	0	0	3
0603_054	1.5	91.7	1.8	1.3	0.5	54.8	35.8	35.8	0.9		1	1	0	0	0	0	3
0603_056	1.0	63.9	1.1	1.0	0.7	66.9	51.3	51.3	1.6	0.9	1	0	2	0	3	3	0
0603_057	1.3	124.0	1.5	4.0	0.9	89.3	21.0	21.0	1.1		3	1	0	0	0	1	2
0603_060	1.3	152.0	1.4	1.3	0.5	103.3	30.2	30.2	1.3		1	2	0	0	2		
0603_179	0.9	64.3	1.2	3.1		74.2	39.0	39.0	1.4		1		0		3	3	0
0603_221	0.9	75.0	1.1	1.9	0.2	80.6	25.0	25.0	1.0	0.9	0	0	1		1	2	1
0603_250	1.9	86.4	1.5	5.9	1.2	48.3	24.0	24.0	1.2		1	1	2	1	0	1	2
0702_007	2.2	116.5		11.6		52.7	22.6	22.6	0.6	1.8	1	0	1		1	2	1
0703_016	1.6	75.7		2.5	1.2	47.4	26.5	26.5	1.3	1.0	3	1	2	2	0	1	2
0703_017	1.6	87.2	2.4	10.6	3.5	53.9	34.2	34.2	1.1		3	2	0		0	1	2
0703_019											1	0	0	0	1	1	2
0703_029	1.2	101.6	1.3	7.3	2.5	92.0	21.0	21.0	0.9	2.3	0	2	0	2		2	1
0703_031	1.4	88.9		13.2	2.0	64.1	27.1	27.1	1.0	0.8	3	2	3	0	0	1	2
0703_035	0.8	70.6	1.6	3.0	0.3	143.3	24.1	24.1	1.6	0.6	1	0	0	0	1	1	2
0703_541	1.2	79.3		1.2		53.7	42.8	42.8	3.5		1	1	0	1	0	2	1
0801_005	1.3	100.2	1.4	2.1	4.0	82.4	45.9	45.9	1.6	0.7	3	0	1		0	0	3
0901_003	1.1	98.6		8.8		97.9	20.4	20.4	1.1	1.2	0	1	0	0		1	2
0901_007	1.2	88.5		9.8	0.8	72.3	38.6	38.6	2.6	2.4	3	2	0	1		1	2
0901_010	1.0	89.4	2.2	57.9	5.6	80.3	21.4	21.4	0.9		3	1	0	0		0	3
0901_012	1.1	79.1	1.4	13.0		77.9	22.3	22.3	0.5	0.1	2	2	0	0		1	2
0901_026	1.1	78.6	1.6	24.4	2.5	69.8	22.5	22.5	1.2	1.0	3	1	0	0		0	3
0901_028	0.9	73.8		1.0		82.5	25.3	25.3	1.0	1.2	1	1	0	0		1	2
0901_031	1.1	114.6	0.9	20.7	2.7	95.3	20.9	20.9	0.7	0.4	2	2	0	0		1	2
0901_033	1.2	89.0		3.8	7.1	73.1	38.6	38.6	1.3	1.1	3	2	1	0		0	3
0901_038	1.3	116.6	1.8	11.2	1.1	91.5	21.5	21.5	1.0	0.6	3	1	0	0		0	3
0901_040	1.0	110.2		2.0		106.2	25.4	25.4	1.2	1.3	3	3	1	0		0	3
0901_055	1.0	77.1	1.5	14.1	2.0	82.9	29.2	29.2	1.4	1.4	0	0	1			3	0
0901_059	1.7	107.7	3.3	15.5	1.7	64.4	20.3	20.3	0.9	0.3	3	1	0	0		0	3
0901_060	1.5	71.9	1.6	2.0		54.9	23.7	23.7	1.2	0.9	0	0	0	0		1	2
0902_081											3	2	1	0	1	1	2
0902_098											1	1	0	0		1	2
0902_113		72.5					30.5	30.5			0	1	0	0		2	1
0902_119													0	0		3	0
0902_125	0.8	87.7	3.2	3.7	0.8	138.2	32.6	32.6	1.6	0.7	3	2	1	1		0	3
0902_131	1.2	83.3	2.0	2.2	1.1	67.4	28.0	28.0	1.6	0.7	3	1	0	0		0	3
0902_139	1.1	74.1	1.2	2.3		71.4	24.1	24.1	1.2	1.1	3	2	2	1	0	0	3
0902_146	1.2	85.6	1.4	4.2		56.4	24.6	24.6	0.8	0.8	2	2	0			2	1
0912_001	1.2	86.7	1.3	28.2	5.3	70.1	19.9	19.9	0.9	0.6	3	2	3	0			
1001_080	1.1	107.2	1.5	5.0	5.0	96.6	23.2	23.2	1.1		3		0	1		0	3
1001_099		71.3					28.0	28.0			3		1	0		0	3
1001_102	1.7	120.6		14.4		67.0	22.4	22.4	1.2	1.4	3			0		0	3
1002_121I						83.0					3	2					
1002_121N	1.1	85.7	2.3	4.0	4.1	70.8	27.9	27.9	1.1	1.3				0		2	1
1002_123											3			0		0	3
1002_124	1.1	79.5	2.3	0.7	2.5	73.7	27.8	27.8	1.2	1.1	1		0	0		3	0
1002_125	1.1	84.4	1.1	1.3	1.0	80.8	23.2	23.2	1.1		3		1	0	0	0	3
1002_126	1.0	137.9	1.2	1.4	7.5	126.5	21.8	21.8	0.9		3		0	0		0	3
1002_127		81.9					20.3	20.3			1			0		1	2

FieldNo_Main	FC_NS_alt	CC_BS	Wind_ES	Sand_ES_rev	Cracks_ES	FI	Weight	dpmkg	dpmkgStd	Saturated	AgeC14Values	AgeC14Std
0101_002	1	2	1	2	3	0.5	0.4588	3.6	0.2	46.4	21.2	1.3
0101_006	0	1	2	3		0.4	0.6916	1.2	0.1	51.1	31.1	1.5
0101_008	0		1	1	2	0.9	0.2742	1.6	0.3	51.1	28.5	1.8
0101_023	1	1	1	1	2	0.2	0.2196	10.9	0.3	46.4	15.8	3.8
0101_049	0	1	2	3	2	1.0	0.3415	6.6	0.2	46.4	16.1	1.3
0101_052		2	1	2	2	1.0	0.33	10.0	0.2	51.1	13.5	1.3
0101_124		2	1	2	2	1.0	0.203	10.1	0.4	51.1	13.4	1.3
0101_133	2	0	1	1	1	1.0	0.256	13.4	0.3	46.4	10.3	1.3
0101_139		3	1	1	2	1.0	0.2781	5.4	0.3	51.1	18.6	1.4
0101_148	0	1	2	3	2	1.0	0.4102	0.3	0.2	51.1	41.2	4.3
0101_151		3	3	0	2	1.0	0.65442	0.1	0.1	46.4	55.8	16.1
0101_153	1	0	1	3	1	1.0	0.2978	1.1	0.2	46.4	31.2	2.2
0101_163	2	2	1	3	2	1.0	0.4999	-0.1	0.1	51.1	49.0	
0102_165		3	1	1	2	0.5	0.4537	0.6	0.2	51.1	36.5	2.4
0102_179		2	1	3	2	0.4	0.4847	0.8	0.1	51.1	34.6	2.0
0102_200	1	2	2	3	2	1.0	0.5326	0.4	0.1	51.1	40.6	3.1
0102_205		3	1	3	2	0.3	0.7098	0.6	0.1	51.1	37.4	2.0
0102_207	3					1.0	0.4808	14.8	0.2	51.1	10.2	1.3
0102_218 (216)		0	0	0	1	1.0	0.5737	26.3	0.2	51.1	5.5	1.3
0102_227	1	1	2			1.0	0.6863	0.8	0.1	51.1	34.0	1.6
0102_231	3	1	1	0	1	1.0	0.5237	8.4	0.2	46.4	14.1	1.3
0102_234	3	0	0	1	1	1.0	0.5725	20.9	0.2	46.4	6.6	1.3
0102_253	0	1	2	1	2	1.0	0.5091	0.7	0.1	51.1	35.9	2.1
0102_256	1	2	2	2	1	1.0	0.4509	0.6	0.2	46.4	36.5	2.6
0102_258	3	1	1	0	1	1.0	0.541	1.8	0.1	46.4	26.8	1.4
0103_259	1	2	1	3	3	0.5	0.6541	9.6	0.1	46.4	13.0	1.3
0201_0077	2	3	1	2	2		0.6016	10.3	0.1	51.1	13.2	1.3
0201_0083	1	2	0	3	0		0.08565	3.4	0.8	55.2	23.2	2.4
0201_0108	0	2	2	3	3		0.4978	0.3	0.1	46.4	41.4	3.9
0201_0135	0	1	3	3	2		0.06105	3.2	1.2	55.2	23.5	3.3
0201_0508	3	1	0	1	0	1.0	0.61772	11.5	0.1	46.4	11.5	1.3
0201_0592		3	2	1	2	1.0	0.81	4.7	0.1	51.1	19.6	1.3
0201_0640	3	2	1	2	2		0.62239	5.8	0.1	51.1	18.0	1.3
0201_0642							0.6807	49.9	0.3	51.1		
0201_0664		0	1	0	1		0.8497	12.8	0.1	51.1	11.4	1.3
0201_0788		2	1	1	1		0.5497	35.4	0.3	51.1	3.0	1.3
0201_0821							0.6596	3.8	0.1	51.1	21.5	1.3
0201_1217	3	1	0	0	1		0.485	25.0	0.2	46.4	5.1	1.3
0209_0004	1	0	2	3	0	1.0	0.681	7.3	0.1	46.4	15.3	1.3
0209_0013	1	0	1	2		1.0	0.695	14.4	0.1	46.4	9.7	1.3
0210_0011	1	2	2	3	1	0.0	0.751	4.9	0.1	51.1	19.3	1.3
0211_0001	0	2	3	1	2	1.0	0.08069	1.5	0.9	55.2	29.9	5.0
0212_0011M	0	2	1	0	1		0.81579	26.1	0.1	46.4	4.7	1.3
0212_1911	0	0	1	3	3	0.3	0.7536	3.4	0.1	51.1	22.5	1.3
0212_1913	1	1	2	3	1	0.7	0.5322	1.7	0.1	46.4	27.2	1.4
0212_1946	3	0	0	2	1	1.0	0.5612	13.9	0.1	51.1	9.1	1.7
0212_1951	3	1	0	0	1	1.0	0.6845	7.9	0.1	46.4	14.7	1.3
0212_1970	0		1	3	3	0.9	0.08458	3.4	0.8	55.2	23.0	2.4
0301_0002	1	1	1	3	2	0.6	2.4	3.0	0.0	51.1	21.6	1.9
0301_0003	3	1	0	0	1	0.5	0.4782	12.7	0.2	55.2	12.1	1.3
0301_0005	0	1	2	3	2	1.0	0.06915	4.5	1.0	51.1	22.3	1.7
0301_0018	0	2	2	0	2	1.0	0.5607	3.7	0.1	46.4	21.0	1.3
0301_0037	0	3	1	3	2	0.1	0.7614	3.1	0.1	51.1	23.3	1.3
0301_0038	3	0	0	2	0	0.9	0.5344	7.6	0.1	51.1	15.8	1.3
0301_0044	1	2	2	3	1	1.0	0.33311	3.9	0.2	55.2	21.9	1.4
0301_0049	0	2	2	3	2	0.9	0.574	0.5	0.1	51.1	38.2	2.4
0301_0050	2	3	1	1	0	1.0	0.7211	5.4	0.1	51.1	18.7	1.3
0301_0061	2	3	1	2	0	1.0	0.6108	10.4	0.1	51.1	13.1	1.3
0301_0066	1	1	1	2	0	1.0	0.451	3.8	0.2	46.4	20.7	1.3
0301_0068	0	1	3	3	3	1.0	0.33647	1.5	0.2	51.1	29.2	1.7
0301_0074	0	0	1	3	2	0.0	0.42227	8.4	0.2	46.4	14.1	1.3
0308_0001	3	1	0	0	0		0.62203	10.3	0.1	46.4	12.5	1.3
0502_031	1	2	1	0	1	1.0	0.10864	2.8	0.6	55.2	24.5	2.3
0502_043	1	2	0	0	2	1.0	0.13222	25.6	0.6	55.2	6.3	1.3
0503_116	1	3	0	1	0	0.6	0.07677	12.2	0.9	55.2	12.5	1.4
0603_021	0	0	2	2	2	0.8	0.07957	8.1	0.9	46.4	14.4	1.6
0603_025	1	0	0	2	2	1.0	0.05937	0.7	1.2	46.4	34.2	13.1
0603_027	0	1	1	3	2	0.1	0.08663	2.0	0.8	46.4	25.9	3.5
0603_028	1	0	0	0	1	1.0	0.08375	2.3	0.8	51.1	25.5	3.2
0603_031	2	0	0	3	2	0.5	0.05979	2.3	1.2	46.4	25.0	4.4
0603_035	2		1	0		1.0	0.08103	20.2	0.9	46.4	6.9	1.3
0603_037		1	2	1	1	1.0	0.09172	9.1	0.8	46.4	13.4	1.5
0603_038	0	1	1	3	1	0.8	0.10903	1.0	0.6	51.1	32.5	5.4
0603_039	1	1	1	1	0	1.0	0.06684	19.6	1.1	46.4	7.1	1.4
0603_041	0	0	2	3	1	0.1	0.08772	0.9	0.8	46.4	32.2	7.1
0603_043	0	0	1	3	0	1.0	0.06487	1.4	1.1	46.4	28.9	6.4
0603_044	0	0	2	3	1	1.0	0.09919	0.4	0.7	46.4	40.0	15.7
0603_046	2	0	0	0	0	1.0	0.06154	32.7	1.2	46.4	2.9	1.3
0603_050	0	1	1	3	0	0.1	0.07641	0.5	0.9	46.4	37.0	13.5
0603_053	0	0	1	1	1	1.0	0.08079	3.3	0.9	46.4	22.0	2.7
0603_054	0	0	1	3	0	1.0	0.07501	>0.5	0.0	51.1	>38	
0603_056	3	1	0	0	1	1.0	0.0725	23.9	1.0	55.2	6.9	1.3
0603_057	1	0	0	3	1	1.0	0.07559	2.3	0.9	46.4	24.9	3.4
0603_060	2	0				1.0	0.05311	>0.5	0.0	46.4	>38	
0603_179	3	0	0	2	0	1.0	0.07994	25.6	0.9	55.2	7.2	0.9
0603_221	2	1	1	0	0	0.9	0.10998	24.5	1.0	55.2	6.7	1.3
0603_250	1	0	1	3	2	1.0	0.09231	3.0	0.8	51.1	23.4	2.6
0702_007	2	2	0	0	0	1.0	0.07572	10.1	1.0	46.4	12.6	1.5
0703_016	1	1	1	3	0	0.5	0.09119	2.5	0.8	51.1	25.0	3.1
0703_017	1	0	0	3	0	1.0	0.09555	2.9	0.8	51.1	23.8	2.7
0703_019	1	2	1	3	2	1.0	0.07531	1.9	1.0	46.4	26.2	4.5
0703_029	2	0	0	2	2	1.0	0.1271	5.3	0.6	46.4	18.0	1.6
0703_031	1	1	1	3	0	1.0	0.08955	1.7	0.8	55.2	28.3	4.0
0703_035	1	1	1	0	1	0.2	0.09372	49.4	2.0	51.1	0.3	1.3
0703_541	2	1	1	0	1	1.0	0.08946	27.7	1.1	55.2	5.7	1.3
0801_005	0	1	2	3	1	0.9	0.11127	1.4	0.7	55.2	30.5	4.4
0901_003	1	0	1	1	1	1.0	0.14658	5.3	0.3	46.4	17.9	1.4
0901_007	1		2	1	0	1.0	0.10607	0.9	0.4	51.1	33.3	3.6
0901_010	0	0	1	3	0	1.0	0.10019	3.1	0.4	46.4	22.4	1.6
0901_012	1	1	1	2	0	1.0	0.11359	7.8	0.3	51.1	15.6	1.3
0901_026	0	1	1	3	1	1.0	0.10759	5.4	0.4	51.1	18.5	1.4
0901_028	1	1	1	1	1	1.0	0.16317	14.1	0.3	51.1	10.6	1.3
0901_031	1	0	1	2	1	1.0	0.10128	18.6	1.0	46.4	7.5	1.4
0901_033	0	0	1	3	1	0.8	0.12504	2.2	0.3	51.1	25.9	1.7
0901_038	0	0	1	3	1	1.0	0.08258	0.7	0.4	46.4	35.0	5.7
0901_040	0	1	1	3	1	1.0	0.088	6.2	0.4	46.4	16.2	1.4
0901_055	3		1	2	0	1.0	0.09638	10.1	0.4	46.4	12.6	1.3
0901_059	0		1	2	1	1.0	0.13628	0.7	0.3	46.4	34.3	3.5
0901_060	1		0	1	1	0.6	0.1078	16.0	0.4	51.1	9.6	1.3
0902_081	1	2	1	2	2	1.0	0.09511	0.4	0.4	51.1	40.1	8.1
0902_098	1	1	0	1	1	1.0	0.12057	5.8	0.3	46.4	19.8	3.4
0902_113	2		1	1	0	1.0	0.09735	14.7	0.7	51.1	10.3	0.2
0902_119	3		1	2	1	0.9	0.09388	19.1	0.4	46.4	7.3	1.3
0902_125	0	1	0	3	1	0.1	0.11465	6.5	0.3	51.1	17.1	1.4
0902_131	0		3	1	0	1.0	0.15211	13.7	0.3	46.4	10.1	1.3
0902_139	0	2	2	3	2	0.6	0.12039	-0.6	0.3	46.4	41.0	
0902_146	2		0	1	1	1.0	0.10725	6.5	1.1	51.1	17.0	1.9
0912_001	0	1	1	3	3	0.2	0.973	1.2	0.1	55.2	32.0	1.4
1001_080	0		2	3	1	1.0						
1001_099	0		1	3	1	1.0	0.9525	2.1	0.1	55.2	26.9	1.3
1001_102	0		2	3		1.0	0.11314	2.6	0.6	55.2	25.3	2.4
1002_121I							0.1043	17.3	0.7	46.4	8.1	1.3
1002_121N	2		1	0			0.09838	20.3	0.7	46.4	6.8	1.3
1002_123	0		2	1		0.9	0.11422	20.3	0.6	51.1	7.7	1.3
1002_124	3		1	2	2	1.0	0.12214	21.0	0.6	46.4	6.5	1.3
1002_125	0	1	2	3	1	0.1	0.1201	11.4	0.6	51.1	12.4	1.4
1002_126	0		1	3	1	0.5	0.17438	-0.5	0.4	51.1	39.0	
1002_127	1		2	1		1.0	0.13351	21.0	0.5	51.1	7.3	1.3

Table S1. Correlation matrix

	14C age	$Wind_{ES}$	$Sand_{ES}$	FC_{ES}	$Salt_{CS}$	$Pore_{CS}$	$Cracks_{ES}$	White $prec._{BS}$	$Green_{BS}$	Red_{BS}	WD	Ba_{ES}	Ba_{BS}	Fe_{CS}/Mn_{CS}	Fe_{ES}/Mn_{ES}	Mn_{ES}/Mn_{CS}	Mn_{BS}	Sr_{CS}	Sr_{BS}	Sr_{ES}	Sr_{ES}/Sr_{CS}
14C age	1																				
$Wind_{ES}$	0.38	1																			
$Sand_{ES}$	0.50	0.26	1																		
FC_{ES}	0.51	0.57	0.49	1																	
$Salt_{CS}$	0.50	0.37	0.60	0.59	1																
$Pore_{CS}$	0.37	0.27	0.36	0.26	0.51	1															
$Cracks_{ES}$	0.30	0.28	0.21	0.28	0.30	0.37	1														
White $prec._{BS}$	0.14	0.24	-0.11	0.01	0.05	0.27	0.26	1													
$Green_{BS}$	0.15	-0.02	0.05	-0.03	0.08	0.21	0.12	0.22	1												
Red_{BS}	0.22	0.20	0.06	0.05	0.18	0.28	0.26	0.43	0.28	1											
WD	0.60	0.35	0.61	0.62	0.66	0.41	0.34	-0.03	0.14	0.09	1										
Ba_{ES}	0.30	0.04	0.11	0.21	0.23	0.14	-0.04	-0.08	0.00	-0.21	0.38	1									
Ba_{BS}	0.29	-0.13	0.03	0.00	0.20	0.22	0.01	0.10	0.40	0.11	0.29	0.32	1								
Fe_{CS}/Mn_{CS}	0.41	0.09	0.21	0.34	0.31	0.16	0.12	-0.25	-0.06	-0.23	0.40	0.29	0.26	1							
Fe_{ES}/Mn_{ES}	-0.25	-0.08	-0.10	-0.03	-0.09	-0.07	-0.03	-0.11	0.05	-0.12	-0.11	0.02	-0.13	0.25	1						
Mn_{ES}/Mn_{CS}	0.42	0.09	0.25	0.20	0.24	0.14	0.16	0.07	-0.07	-0.04	0.34	0.38	0.25	0.31	-0.61	1					
Mn_{BS}	0.50	0.17	0.33	0.21	0.36	0.27	0.38	0.23	-0.14	0.12	0.41	0.29	0.13	0.04	-0.62	0.71	1				
Sr_{CS}	0.30	0.10	0.27	0.24	0.30	0.16	0.25	0.10	-0.02	0.01	0.29	0.10	0.04	0.24	-0.05	0.14	0.37	1			
Sr_{BS}	0.14	-0.03	-0.02	0.04	0.00	0.04	0.05	0.06	-0.18	-0.21	0.07	0.09	0.11	0.25	-0.13	0.32	0.19	0.22	1		
Sr_{ES}	0.24	0.14	0.21	0.17	0.26	0.28	0.18	0.07	-0.03	-0.09	0.36	0.34	0.19	0.30	0.05	0.38	0.49	0.36	0.58	1	
Sr_{ES}/Sr_{CS}	0.04	0.03	0.08	-0.01	-0.07	0.03	-0.16	0.03	-0.12	-0.08	-0.07	-0.08	0.03	0.05	0.14	-0.07	-0.13	-0.27	0.34	0.41	1